

[Click here to view linked References](#)

Laboratory X-ray micro-computed tomography: a generalised approach for biological samples using a three-horned chameleon as example

Anton du Plessis^{1,2, a*}, Stephan Gerhard le Roux^{1,b} & Anina Guelpa^{1,c}

¹ CT Scanner Facility, Central Analytical Facilities, Stellenbosch University, Stellenbosch, South Africa

² Physics Department, Stellenbosch University, Stellenbosch, South Africa

^a anton2@sun.ac.za, ^b lerouxsg@sun.ac.za, ^c aninag@sun.ac.za

* Corresponding author

Abstract

This paper provides a detailed “how-to guide”, describing many important concepts for users of micro-computed tomography (micro-CT) facilities to consider when planning their work. In this process the method is described in technical detail, explaining the important choices with regards to scan setup and parameters. A unique three-horned chameleon is presented, which was scanned at different resolutions and accompanied by simple analysis. Full data sets of this three-horned chameleon are provided as supplementary information. The aim is for new users to gain experience in working with typical micro-CT data and to be able to view analysis results in 3D. Besides being a fascinating test sample, this species of chameleon has not been analysed in such detail before. It is important to note that the technical detail and discussion is relevant to all commercial types of micro-CT instruments and we hope this paper will assist researchers in making better use of this powerful and emerging technology.

Keywords: Industrial CT, X-ray tomography, micro-computed tomography, nano-computed tomography, 3D imaging, non-destructive testing, three-horned chameleon

1. Introduction

The ability to perform non-invasive analysis is often of prime concern when working with biological samples. Therefore, much attention has been given to find techniques for the inspection of internal properties or the evaluation of quality attributes from biological samples, non-destructively. One such technique, computerised axial tomography (CAT) or medical computed tomography (CT), is widely used for non-destructive imaging of the internal organs and structures of the human body [1]. Generally, this method involves the recording of two-dimensional (2D) X-ray images from various angles around an object, followed by digital three-dimensional (3D) reconstruction. More generally, CT can refer to any form of penetrating radiation being used to record 2D images of any object from different angles followed by reconstruction of these images using digital algorithms, into a 3D data set. Thereby, the data from CT results in a virtual rendering of the object under investigation. This allows one to virtually travel through the volume in any direction and angle, view selected internal features, or make dimensional or volumetric or other more advanced three dimensional measurements [2, 3].

Industrial X-ray computed tomography is a specialised form of CT scanning meant specifically for non-medical applications (hence the term industrial) and frequently involves resolutions in the micro-meter scale. The method is therefore termed micro-computed tomography (micro-CT) and in the case of sub-micron resolution, such methods are termed nano-CT or sometimes X-ray microscopy, as the resolution is similar to optical microscopes. Other terms in general use are X-ray CT (XCT), industrial CT, and laboratory X-ray tomography. Industrial CT differs from medical CT in two major ways: firstly, the resolution is potentially much improved and variable in micro-CT systems, due in part to the stable fixed source and detector and a rotating sample (in contrast to medical CT where the sample is stationary and the source and detector move around it); and secondly, industrial CT is not dose-limited and have a wide variety of choices with regards to voltages, currents and beam filtration. X-ray micro-CT systems can also vary considerably in system capabilities, from small low-cost benchtop systems to cabinet systems able to house larger samples and even as large as walk-in cabinet systems with multiple X-ray sources. Similarly, different manufacturers provide different hardware and software options. These systems should not be confused with synchrotron CT, where synchrotron radiation is the X-ray source, as opposed to laboratory generated X-ray radiation [4]. Synchrotron CT differs from laboratory CT as it has much higher brightness X-ray radiation, allowing much shorter scan times for similar or better quality, and allowing higher resolution on larger sample sizes than laboratory CT. However, synchrotron CT is not as widely available or as easily accessible as laboratory CT and such work must be planned months in advance. Since laboratory CT is available widely, in some cases in open access format, planning is limited to weeks or even days.

63 X-ray micro-CT has numerous applications and is useful in any scientific field where non-
1
2 64 destructive analysis is required. The versatility of this technique is shown in the number of reviews
3 65 that have been published recently, such as in food sciences [5], the geosciences [6], biology [4] as
4
5 66 well as materials sciences [7, 8].
6
7 67

8 68 Despite its numerous applications and potential, the method is still underutilised as new users
9
10 69 struggle with the mystery that surrounds the entire scanning process, including sample
11
12 70 preparation, scanning, reconstruction and choices for analysis types. Lack of knowledge regarding
13 71 the mentioned processes could result in poor scan quality, inefficient use of facilities or the inability
14
15 72 to extract required information for the required research purpose. Some work has been published
16
17 73 in a book chapter focusing on bone microstructural analysis, where details of the CT scanning
18 74 process have been outlined to assist in de-mystifying the process, especially for new users to the
19
20 75 technique [9]. A similar work was presented by Mizutani and Suzuki [4], where the focus was on
21
22 76 soft tissue scanning and staining methods to enhance contrast. In the present data note, we focus
23 77 on new users from general biological backgrounds and present a multi-scale investigation of a
24
25 78 three-horned chameleon specimen. We add the full data sets of the chameleon scanned at 75 μm ,
26
27 79 30 μm , 10 μm , 4 μm and 0.95 μm , to aid new users and researchers who might not have access
28 80 to funding for obtaining their own micro-CT data sets. Hopefully this work will lead to more
29
30 81 effective use of micro-CT facilities, through an improved understanding of the capabilities and
31
32 82 limitations of the technique.
33
34 83

35 84 **2. Background to computed tomography**

36
37 85 X-ray micro-CT as a technique makes use of information from projected 2D images as obtained by
38
39 86 a X-ray source and a detector to investigate the internal structure of a sample [10]. The
40 87 fundamental components of any micro-CT instrument are (1) penetrating ionising radiation, (2) a
41
42 88 sample manipulator and (3) a detector [11] (Fig. 1). The basic principles of X-ray micro-CT are
43
44 89 generally described in Kak and Slaney [12]. X-rays are generated using a micro-focus X-ray tube,
45 90 which uses a beam of electrons accelerated by a voltage of up to 240 kV or more in a vacuum
46
47 91 tube, and are focused onto a tungsten metal target (or other metal target material, though
48
49 92 tungsten is most widely used). The fast moving electrons hitting a metal target material creates X-
50 93 rays. In a micro-focus X-ray tube the resulting cone beam of X-rays is directed through and around
51
52 94 a sample, before being collected on a 2D X-ray detector in the form of a “shadow image”, also
53
54 95 called a projection image or radiograph [3]. The sample manipulator (or rotation table) positions
55 96 the sample in the path of the radiation beam and rotates it through a specific angle (usually 360°).
56
57 97 The detector converts the attenuated radiation, which passes through the sample along a straight
58
59 98 line, into the 2D digital images, consisting of thousands of pixels. In this way, many hundreds or
60 99 thousands of 2D projection images are recorded during the scan process. After scanning, these
61
62 100 images are used to reconstruct a three dimensional data set by making use of filtered back-
63
64
65

101 projection algorithms [13]. Effectively, every volumetric pixel (or voxel) was imaged (by 2D
102 projections) from many angles, and the sum of its view from every angle produces a good
103 representation of the actual X-ray density and hence brightness of that voxel [3]. Following
104 reconstruction, data visualisation and analysis is possible using a variety of software tools, some
105 more complex than others. These steps are all described below with discussion of practical
106 considerations.

107
108 Insert Figure 1 approximately here

109 110 3. Computed tomography (CT) basics

111 The steps associated with X-ray micro-CT include: set-up considerations (sample preparation and
112 mounting, sample size vs. resolution, step positions and averaging, voltage settings, filtration of
113 beam and detector and penetration ratio), scanning, reconstruction, visualisation, image
114 processing and analysis, as well as further scanning at higher resolution. These steps will be
115 explained, where applicable, by means of an example: a three-horned chameleon, the Jackson's
116 chameleon (*Trioceros jacksonii*) (Specimen number USEC/H-2927 from the Stellenbosch
117 University Zoology/Botany Department's collection) scanned using a Phoenix V|Tome|X L240
118 (General Electric Sensing and Inspection Technologies / Phoenix X-ray, Wunstorf, Germany)
119 micro-CT system, as well as a Phoenix nanotom S (General Electric Sensing and Inspection
120 Technologies / Phoenix X-ray, Wunstorf, Germany) nano-CT system, both located at the CT
121 Scanner Facility of the Central Analytical Facility (CAF), Stellenbosch University, South Africa
122 (<http://blogs.sun.ac.za/ctscanner/>).

123 124 3.1 Set-up considerations

125 A scan set-up involves a good choice of parameters based on some general guidelines,
126 experience with different sample types and requirements of the analysis. Five general guidelines
127 (*Guidelines I to V*), along with explanations will be presented in this section for careful
128 consideration when performing micro-CT measurements of biological samples.

129 130 3.1.1 Sample preparation and mounting

131 Amongst analytical techniques, micro-CT requires very little, if any, sample preparation. Generally,
132 a sample can be scanned exactly as provided, without any sample preparation. However, staining
133 is sometimes necessary when poor material discrimination is found, i.e. biological soft tissues. X-
134 ray specific staining (or labeling) is performed with contrast media (iodine or barium or many
135 others) [4]. Briefly, a sample can be soaked in a contrast agent (such as a liquid solution
136 containing iodine) for a period of time and then removed, dried and mounted for micro-CT
137 scanning. Staining is not something that should be attempted as a first experiment, and should
138 only be used in special cases and when all other options have failed to improve contrast.

139
140
141
142
143
144
145
146
147
148
149
150
151
152
153
154
155
156
157
158
159
160
161
162
163
164
165
166
167
168
169
170
171
172
173
174
175

To obtain best scan quality it is important to load the sample properly. Samples should be loaded at a slight angle to ensure that parallel surfaces to the X-ray beam are minimised. Parallel surfaces are not penetrated properly and lead to image artifacts and lack of detail in the data set in the plane of the flat surface parallel to the beam.

The mounting involves a low-density material (cardboard tubes, plastic bottles or glass rods) which holds the sample in place on a rotation stage (turntable), but separates the sample from the dense rotation stage hardware. The most important parameter in a good scan is ensuring that the sample does not move during the scan time. This is more relevant for longer scan times. If a sample suddenly moves due to mounting tape coming loose during the scan, it will result in a blurred 3D image. In the same way, a wet sample that dries out during the scan (causing shrinking) will also cause a blur. For wet samples, such as biological preserved specimens, there are different approaches that can be used to overcome this problem. One approach is to dry the sample before scanning, or to make use of freeze-drying. Another approach is to wrap the sample in a wet cloth, thereby keeping the sample wet for an adequate period. It is also possible to scan samples inside liquid filled tubes, although it can be challenging to keep the sample in place. Additionally, if it is kept in place by the edges of the container, these edges will not be separable from the sample in the image processing steps. Another approach to minimise blurring is to use very fast scan settings, although this is not always possible when highest quality and resolution is required.

Some mounting options are presented in Figs. 2a, 2b and 2c, respectively showing a specimen covered with a wet cloth, mounted upright for vertical, multiple-part scanning, and lastly, a nano-CT mounting. The wet-cloth mount is useful for keeping a sample wet during a scan, and is useful when only the internal features are of interest, since the cloth and the skin of the sample are not digitally separable in the scan data. The vertical mounting method is useful when multiple-scans at higher resolution are done of different sections along the height and then stitched together to form a higher resolution complete data set. The nano-CT mounting is also used in similar form as with micro-CT of smaller samples, where a glass rod is used and the sample is mounted on top of this rod with double sided tape, glue or using a small cube of foam stuck to the rod. Other options include rigid foam stuck to the top of a glass rod, fitted with a small cavity or slit, plastic film covering soft tissue or wet samples and soft foam for wrapping a sample placed on top of the glass rod.

Insert Figure 2 approximately here

3.1.2 Sample size vs. resolution

176 Micro-CT instruments can accommodate sample sizes from as large as 40 cm (or larger in some
177 systems) to as small as several micrometers [6]. Large walk-in cabinet systems allow the detector
178 to back up as far as 1.6 m from the X-ray source, which allows samples as large as 40 cm to be
179 loaded and fit within a single scan volume, with the usual single scan volume covering
180 approximately 30 cm at its furthest position. Smaller cabinet micro-CT systems allow generally a 1
181 m source-detector distance allowing up to 15 cm in a single scan. Benchtop instruments have
182 further limitations on sample size and might require sectioning of samples in the preparation
183 process, although this may not always be a drawback since benchtop instruments are lower cost
184 and more readily available than larger systems.

186 The choice of resolution is the first major factor affecting a micro-CT scan. Useful guidelines
(*Guideline 1*) when estimating the best possible resolution for a sample of known dimensions are:

- i. The best commonly used resolution is a factor 1000 smaller than the width of the sample.
This means for a sample 100 mm wide, the best resolution is typically 100 μm

The above guideline is based on the standard practice of using only the central 1000 of 2000
available pixels of the detector to minimise possible artifacts from the edges. Most detectors have
2000 pixels but some systems have more, which allow improved magnification for the same
sample size, but might introduce other problems such as data set size and long reconstruction
times. It is in theory possible to use all 2000 available pixels in the above example, in which case
up to 50 μm is possible. However, besides the potential for artifacts from the edge regions, it is
practically very difficult to mount a sample perfectly central on the rotation axis in order for it not to
move out of the field of view during a rotation, and this process could also be very time consuming
at high resolution.

These guidelines are generally applicable to most modern micro-CT instruments, which typically
have 2000 detector pixels and a graph depicting resolutions obtained vs. sample sizes is
presented in Fig. 3. In general, resolutions of micro-CT scanners are in the range of 5 – 150 μm
(0.005 to 0.15 mm), compared to medical CT scanners having best resolutions of 0.7 mm.
Generally, nano-CT scanners have resolutions down to 0.5 μm (500 nm) in laboratory instruments
(some higher resolution instruments are available, but not widely available yet).

Insert Figure 3 approximately here

3.1.3 Resolution, voxel size and X-ray spot size

The voxel size of a micro-CT image is dependent on the magnification and object size as
described above. This is related to the distance of the sample from the X-ray source and the

214 detector [5]. Voxel size and spatial resolution are two concepts that are often confused, since the
115 voxel size is the size of a pixel in 3D space, i.e. the width of one volumetric pixel (isotropic in 3
216 dimensions). This value does not consider the actual spatial resolution capability of the scan
4 system. If the X-ray spot size becomes larger than the chosen voxel size, the spatial resolution of
317 the system becomes poorer. Since most commercial systems limit the size of the X-ray spot to the
618 required voxel size (or provide the user an indication of this), the actual and voxel resolution are
819 usually the same, but this is not generally tested or reported. It is possible to use resolution
1020 standards (such as calibrated-thickness metal wires) to confirm spatial resolution and some
1121 reference standards exist although a generally accepted standard for industrial CT systems does
1322 not exist. It is therefore possible that the amount of detail that is detectable in a scan can vary
14 considerably from system to system, or even between different scans from the same type of
1623 system. This is due to improper settings that possibly result in large X-ray spot sizes, or due to
1724 improper choice of other scan parameters.

21 When scanning an object at different resolution settings, the same object with a better resolution
227 (higher magnification) will cover a larger portion of the detector resulting in more angular positions
2328 required for a good reconstruction. This affects the total scan time, making a higher resolution
24 more time consuming. This factor is discussed in the next section in more detail.

31
3233 3.1.4 Scan time, number of images and rotational options

33 The major consideration for scan time is the acquisition time of single projection images, which
34 can vary from system to system due to detector sensitivity and dynamic range differences, X-ray
35 tube brightness differences, and differences in physical distance from source to detector [3]. A
36 typical image acquisition time in a walk-in cabinet system with a 16-bit flat-panel detector is 500
37 ms per image, while some benchtop systems have typical image acquisition times of 2000 ms per
38 image. All systems have variable image acquisition times and therefore scan times can vary
39 considerably. For highest possible quality scans, keep in mind to make full use of the dynamic
40 range of the detector. In doing so, the image contrast is maximised by raising the image
41 acquisition time up to near saturation of the detector for a particular X-ray setting. If the image
42 acquisition time is too low, the resulting contrast will be poor with grainy images in extreme cases.

50 Some scanners involve continuous scanning (continuous rotation and image acquisition without
51 steps), but the discussion here is limited to a stepwise rotation for simplicity. At each step position,
5245 one or more images can be acquired and averaged to provide an improved image quality
53 (compared to a single image per position). Averaging reduces noise and therefore improves image
54 quality, but its effect depends on the inherent noise of the detector used. For samples which may
55 have small vibrational movements during rotational movement, e.g. leaves or hairs, it is advisable
56 to use the skip function if available, which ignores the first image acquired at each new step

252 position (during which time the sample stabilises). Since this vibration is due to the stepwise
1
253 process, another approach is to use continuous scanning which also reduces vibration but in that
2
254 case averaging is not possible.
4

255
5
256 Generally, the number of step positions required depends on the sample size relative to the
7
257 magnification. Therefore, the higher the magnification and hence the number of pixels used on the
9
258 detector, the larger the number of images required for a good reconstruction.

11
259
12
13
260 A useful guideline in this regard (*Guideline II*) is:
14

- 15
16
261
17
262 i. The number of pixels covered by the sample on the detector in width multiplied by 1.6
18
263 equals the number of projection step positions required. Consequently up to a maximum of
19
264 3200 step positions are used for a typical 2000 pixel wide detector.
21

22
265
23
266 This important concept therefore plays a large role in scan time determination.
24

25
26
267
26
268 3.1.5 X-ray parameters: voltage, penetration values and background intensity

28
269 X-ray projection images or radiographs can be viewed live and can be used for non-destructive
29
30
270 analysis without the use of 3D reconstruction. In fact this method of “digital radiography” is in wide
31
32
271 use for industrial non-destructive testing purposes [14], though it is limited for complex objects and
33
272 does not provide depth information, e.g. the presence of a void can be determined but not how
34
35
273 close it is to the surface or how close to other features in the line of sight. It is sometimes useful to
36
37
274 use the live digital X-ray projection image as a fast scout method to quickly assess the inside of an
38
275 object, thereby determining if a full CT scan is necessary (to provide a more detailed 3D view). An
39
40
276 example of an X-ray projection image of the chameleon is given in Fig. 7b.
41

42
277
43
278 For CT scan setup, the radiograph or projection image is used as a basis for selecting good X-ray
44
45
279 parameters, based on the sample’s penetration values and the background intensity values.
46
47
280 Different types of samples require different X-ray voltages for best quality and this cannot always
48
281 be predicted or estimated before a scan. The best possible material discrimination is obtained by
49
50
282 using lower voltages. However, if a dense object is present, the X-ray penetration will be
51
52
283 insufficient (sometimes unexpectedly) causing noise and artifacts. Beam hardening is the most
53
54
284 common CT artifact and occurs due to the fact that the X-ray beam is polychromatic, with a range
55
285 of low and high energy X-rays present, and because low energy X-rays are absorbed more easily
56
57
286 than high energy X-rays. This results, for dense objects, in differences in absorption from different
58
59
287 angles resulting in streaky artifacts across the image in the 3D data set.

289 If too high voltage is used, very poor contrast is obtained between different materials. These
1 290 factors are important for a proper choice of scan parameters but also for sample preparation. For
2 291 example, consider the scan of a biological museum specimen (preserved small animal) with a
3 292 metal name tag. It is better to scan such an object without its metal name tag, than with it. The
4 293 metal is much denser for X-ray penetration than the sample itself, resulting in beam hardening
5 294 artifacts at the best (low voltage) settings for the scan. By increasing the voltage, this limitation can
6 295 be overcome and the metal tag can be scanned properly, but with a major reduction in quality of
7 296 the image of the biological specimen. Fig. 4 shows examples of scans of the chameleon (a) with a
8 297 metal tag in the scan resulting in streaky artifacts (b) at too low voltage causing some minor
9 298 artifacts around dense internal features and (c) at too high voltage showing poor contrast.

16 299
17 300
18 301
19 302
20 303
21 304
22 305
23 306
24 307
25 308
26 309
27 310
28 311
29 312
30 313
31 314
32 315
33 316
34 317
35 318
36 319
37 320
38 321
39 322
40 323
41 324
42 325
43 326
44 327
45 328
46 329
47 330
48 331
49 332
50 333
51 334
52 335
53 336
54 337
55 338
56 339
57 340
58 341
59 342
60 343
61 344
62 345
63 346
64 347
65 348

Insert Figure 4 approximately here

301 The choice of voltage is strongly related to the sample type and the goal of the scan, but some
302 general guidelines (*Guideline III*) are as follows:

- 303 i. biological samples: 30 to 100 kV;
- 304 ii. small rocks and light metals: 60 to 150 kV;
- 305 iii. heavy metals (e.g. steel) and larger rocks: 160 to 240 kV or more; and
- 306 iv. in general: the smaller a sample the lower the voltage that is possible.

307 When the voltage is increased, it is often useful to add beam filters to pre-compensate for beam
308 hardening and effectively reduce the polychromaticity of the beam, thereby preventing streaky
309 artifacts. Commonly used filters include from 0.1 up to 2 mm of copper and from 0.5 to 1.5 mm tin
310 or combinations of these. Other beam filters can be used, such as aluminum that is a popular
311 choice. The selection of beam filters is usually more relevant to very dense objects and not
312 biological samples. In the case of most biological samples no beam filtration is required or when
313 required, at most 0.5 mm copper or aluminum. Detector filtration (using a filter between the object
314 and detector) can also be used in specialised cases to reduce noise, for example where the
315 sample produces secondary X-ray emission, especially when very dense objects are scanned, or
316 when a large amount of scattering is present.

317 *Guidelines IV* are presented for the determination of adequate penetration values:

- 318 i. A typical setup method to find best settings for a particular sample type, is to rotate the
319 sample until its 2D X-ray projection image shows the darkest region (its longest or densest
320 axis) and then to calculate the sample's minimum penetration ratio compared to the
321 background X-ray intensity (using the grey value counts measured in the X-ray image).
- 322 ii. If the penetration value is less than 10%, an increased voltage or current is required.

- iii. However, this might cause the detector to saturate, in which case beam filters can be applied to prevent saturation, while still increasing the penetration value.
- iv. By using a beam filter, a higher voltage or current can be obtained with a reduction in the low energy X-rays such that the detector does not yet saturate.
- v. Penetration values from 10 % to 90 % should result in good scan quality.
- vi. In order to reduce penetration, lower voltages should be used.
- vii. Since X-ray emission is typically very limited below 50 kV, longer scan times are then required to obtain large enough signals.

3.1.6 Scan quality problems and artifacts

As can be seen above from the many variations of scan settings, different quality scans can be obtained. Figs. 5 shows micro-CT slice images of the chameleon with poor contrast, double edge and slight blur, respectively. These are typical image quality problems that can occur. In particular, Fig. 5a has poor contrast, in this case due to incorrect reconstruction setting (clamping) which will be discussed in Section 3.3. The same effect will occur when scanning a sample with the metal rotation table in the scan volume, or when too low voltage is used. Fig. 5b has a double edge due to incorrect reconstruction setting (offset correction) which will also be discussed in Section 3.3. The same type of double edge will occur to a lesser degree if the sample moves during a scan. Fig. 5c shows only a slight blur on the edges, which is due in this case to hardware misalignment, where the rotation axis of the sample and the X-ray tube direction is slightly more or less than 90 degrees (referred to as the tilt axis). These images are meant to demonstrate typical image quality problems.

Insert Figure 5 approximately here

Beam hardening was already mentioned above when discussing choices of voltages, within the context of streak artifacts. However, for homogenous dense objects scanned with too low voltage, a “cupping” effect is also possible where the edge of the sample seems brighter than the inside. This artifact is present when insufficient penetration of the sample is obtained, for example due to too low voltage. Other artifacts and unwanted image effects include cone beam artifacts affecting the edges of materials near the edges of the detector, double edges due to tilt axis misalignment relative to beam axis, and blurring due to unstable rotational axis.

3.2 Scanning

Before a scan commences, the background must be normalised by removing the sample and using the X-ray beam at the chosen settings, and correct for all intensity variations across the detector (e.g. the beam is more intense in the middle than the edges of the detector, but the normalised pixel intensity must be equal for a good scan). This normalisation or correction process

365 can be done before every scan, but is only required if X-ray or acquisition settings change, or at
1
366 the start of a day of scanning, for example. It is also necessary to run a beam centering right
2
367 before scanning to ensure the electrons are well focused resulting in optimal X-ray output.
4
368

6
369 Once the sample is loaded and settings chosen, a scan can be acquired. The scanning is done
7
370 automatically with no user interaction, but errors can occur during the scan, requiring frequent
8
9
1071 supervision. For example, the X-ray source could become unstable requiring warmup, the filament
11
1272 could burn out requiring replacement, or other errors could occur requiring attention to either
13
1473 continue the scan as soon as possible, or re-start the scan once the problem is solved.
14

16
1775 Due to long scan times, the potential for low image quality or artifacts and the requirement to find
18
1976 optimal settings for particular sample types, or due to large numbers of samples requiring
19
2077 scanning, fast scans are sometimes required. Such fast scans (e.g. 15 min) are not ideal, but can
21
2278 be sufficient for some purposes, such as identification of relatively large features, finding regions
23
2479 for further analysis or for higher quality scanning, or for simple measurements. Such fast scans
24
2580 can also be used as a scout method, to find a region of interest for a long, high quality scan.
26

28 2982 3.3 Reconstruction

3083 Reconstruction entails the creation of a 3D data set from 2D image projections and different
31
3284 options are available, as well as different data output types, as presented in this section.
33

35 3686 3.3.1 Reconstruction options

3787 After a full scan, the data is reconstructed which refers to creating a discrete 3D data set from 2D
38
3988 image projections. Sometimes a reconstruction refers to a 3D image rendering or visualisation of a
40
4189 3D data set, but we call this instead “visualisation” and describe this in the next section in more
41
4290 detail. The reconstruction process involves effectively the mapping of each voxel, by using
43
4491 projection image representations of that particular voxel from many angles. This mapping is done
45
4692 by a Feldkamp filtered back-projection algorithm [15]. Commercial micro-CT systems all have
47
4893 built-in reconstruction software packages with slightly different available settings but all based on
48
4994 the same algorithms. General Electric uses a software called Datos. Volume Graphics is a stand-
50
5195 alone software package mainly used for 3D image analysis but also offers a module for
51
5296 reconstruction which is very similar to Datos, and another commercial standalone software for
53
5497 reconstruction is offered by Inside Matters, called Octopus Reconstruction.
54

55
56
5799 Reconstruction software involves a series of choices or options, which can also affect the quality
58
5900 of the obtained 3D data. These options will be described in general here, though not all options
60
6101 are available in all reconstruction software packages.
61

- 402 i. Firstly, the field of view can be cropped to make the total reconstructed volume smaller.
403 This helps reducing the data set size and makes reconstruction faster since less memory is
404 required, especially helpful when time or computing power is limited.
- 405 ii. A choice of data type can be made which is usually selected as 16-bit, but 8-bit can be
406 selected if storage space or memory is a problem.
- 407 iii. The exact location of the rotation axis in each projection image is found by making use of
408 an automated algorithm which finds the central pixels in all 2D X-ray images – the use of
409 the exact rotation axis in the back-projection algorithm improves the quality of the
410 reconstruction and is especially important at higher resolutions.
- 411 iv. This process can also be coupled with a refinement process correcting for small movement
412 or shift of the sample or due to inaccuracy of the rotation stage. This can be done by
413 viewing before-after projection images and correcting for any small shifts. In advanced
414 software packages, this can be done at more than one position during the scan, correcting
415 for changes which occur at different times during the scan. This process is limited to very
416 small changes but does result in much improved edge clarity in the reconstructed data set.
- 417 v. Another important choice is beam hardening correction, which corrects much of the
418 generally-occurring “cupping” effect in samples where the edges seem brighter than the
419 middle of the scan. This can be attempted by trial and error until the best value is found
420 (values can be chosen in a range from light to heavy implementation of the algorithm).
- 421 vi. Another option sometimes available, is when it is possible to disregard a certain % of pixels
422 that are “outliers” in terms of strong or weak absorption compared to the rest of the data,
423 which effectively improves the grey value contrast in the images. This is called “clamping”
424 and can be very useful when a small quantity of bright dense phases are present but are
425 not of interest, and are therefore all grouped as the same brightest grey value. The % of
426 pixels that are clamped, and the clamping direction (lowest or highest grey values only, or
427 both) can be set.
- 428 vii. It is also possible to make use of special settings to select the background detector counts
429 in each image and normalise this across the series of images, which is useful when
430 scattering is present resulting in brighter or darker projection images from different angles.
- 431 viii. It is possible to use special algorithms to remove ring artifacts by disregarding “dead” pixels
432 from the 2D projection images. Ring artifacts especially near the center of rotation are also
433 removed by making use of a detector shift process whereby the detector shifts horizontally
434 between step positions and which are corrected in the reconstruction process resulting in a
435 smoothing of the rotational center artifact.
- 436 ix. It is also possible in region-of-interest (ROI) scans (where the sample extends over the
437 sides of the 2D image), to remove the bright ring which results around the outside of the
438 scan volume and hence improve the image quality by using a special algorithm dedicated
439 for this purpose.

440
1
2
3
4
5
6
7
8
9
10
11
12
13
14
15
16
17
18
19
20
21
22
23
24
25
26
27
28
29
30
31
32
33
34
35
36
37
38
39
40
41
42
43
44
45
46
47
48
49
50
51
52
53
54
55
56
57
58
59
60
61
62
63
64
65

Therefore, it is clear that many different possibilities exist for reconstruction and hence this process is in itself an important step, which can assist in obtaining improved image quality even when using lower cost CT scan hardware. Since the reconstruction process itself can vary significantly, it is suggested to retain X-ray projection images even when reconstruction has been completed, thereby allowing future improved reconstruction of the same data, where possible.

In medical CT, each voxel is typically associated with a calibrated Hounsfield Unit or CT number, which is regarded as the average attenuation in that section of the sample [16]. However, in micro-CT the grey values are not calibrated and depend on reconstruction settings in the software used, as well as various scan parameters. In general, therefore the reconstructed data from micro-CT scans are not calibrated for density determination.

It is also possible to use resolution reduction or oversampling in the reconstruction process, as well as filtering of the 2D projections using a variety of image filters. These are not standard and only used in specialised cases. Another seldom used option is to reconstruct scans of less than 360 degrees, when a sample is too large to rotate fully in the system used, for example. It can be mentioned here that in the case of data collection, sometimes an image could get corrupted or lost. A simple process of replacing this image with its adjacent image in the sequence, results in a good reconstruction, even though an image may be missing.

Insert Table 1 approximately here

3.3.2 Data output types

Both the X-ray projection images captured by the CT system and the reconstructed CT dataset consist of pixels or voxels which have specific shades of grey. Each of the pixels or voxels are assigned a specific value which indicates the intensity of its shade of grey. These values differ depending on the bit depth assigned to it e.g. 8 bit = $2^8 = 256$ which indicates the grey value range (in integral values) is from 0 to 256 and 16 bit = $2^{16} = 65536$, which indicates that the grey value range is from 0 to 65536. The advantage of the 16 bit dataset over the 8 bit dataset is that it has more capacity to differentiate between small density changes because of the larger grey value range providing a more accurate representation of the sample that was scanned. In general commercial micro-CT scanners have detectors with dynamic range of between 12 and 16 bit, so using 8 bit data sets result in loss of information. The advantage of 8 bit data types is the much smaller physical size (50% reduction) and hence easier handling for visualisation, analysis and transfer of data.

477 A general comment about image file types is warranted here. There are different image files types
1
478 with the main difference being JPG and BMP and similar which are Windows compressed image
2
479 formats and TIFF which is uncompressed. The compressed file formats are lower quality and can
4
480 results in loss of information. Though the use of a compressed file format can reduce data set
6
481 size, it is advised to rather use poorer resolution scans to reduce data set size. In order to achieve
7
482 this, during the setup step, the sample is moved back such that it fills less of the field of view of the
9
1083 detector which will result in a smaller data volume (and shorter scan time). Also worth mentioning
11
1084 is that 16-bit TIFF files cannot be viewed properly by windows image viewer programs. High
12
1085 quality image viewing programs such as Irfanview are required.
14

1586
16
1087 Image stacks are calibrated in the sense that each isotropic voxel has a side length equal to the
17
1088 scan's voxel size. However, post-processing of this data and creation of images for viewing,
19
2089 including scale bars, do not necessarily maintain this pixel spacing, especially when creating lossy
21
2090 file types such as JPG. The original image stack must therefore be kept together with knowledge
22
2091 about the voxel size. In some scanner types this information, together with all scan settings, are
24
2092 kept in a file which can be read in notepad (e.g. PCA file in General Electric Phoenix systems or
26
2093 TXT file in Nikon systems). Saving image stacks with a scale bar from image processing software
28
2094 is not suggested for two reasons: firstly, these scale bars are not accurate enough (rounded off)
29
3095 and secondly, having a scale bar in a slice image creates a long 3D scale bar, which is not useful.
31

33 34 3.4 Visualisation

3598 Typically, volume analysis and visualisation is done in a 3D data analysis software package.
36
3499 These differ from 3D Computed Aided Design (CAD) software in that they handle full voxel data,
38
500 i.e. data exist everywhere in a 3D voxel grid, not only on surfaces of the object. In other words,
39
4001 CAD software packages use triangulated mesh data of surfaces only (point locations only), while
41
4002 full CT data comprises data at every point in 3D space (grey value at every point). Therefore, a
43
4003 volumetric data set is significantly larger and requires more intensive computing power, even for
44
4004 simple visualisation. Commonly used software available for volume rendering include Avizo,
46
4005 Volume Graphics VGStudio, ImageJ, Blob3D and Simpleware, whereas surface rendering
48
4006 software are AutoCAD, Blender, SolidWorks and Autodesk. Additionally, open source software
50
5007 which can be used for analysis of CT data in 2D or 3D include ImageJ, MIPAR, Blob3D, Quant3D
51
5008 and 3dma_rock.

53 509 55 3.5 Image processing and analysis 56

5711 The most widely used step in 3D image processing is thresholding. This involves in the simplest
58
5012 case, a selection of a threshold grey value such that all grey values in the volume brighter than this
60
5013 value is selected for viewing or further analysis. This method uses the same threshold across the
61
6014 entire volume and is therefore called global thresholding. Besides this simple thresholding step,
63
64
65

515 individual features may be highlighted and analysed in detail with regards to its 3D location in the
516 animal. Aligning the slice image to the feature allows the viewing in the correct plane, which is a
517 useful feature for visualisation of different components from different angles in slice images. Its
518 selection was done using a region growing tool, i.e. a voxel is selected inside this feature and all
519 connected voxels with similar grey values assigned to this region of interest. This region can be
520 visualised alone or its colour chosen as demonstrated here, different from the rest of the animal. It
521 is possible to view this in 3D rendering as well by making the rest of the animal semi-transparent
522 and the feature of interest non-transparent. A basic typical image processing procedure is
523 described below but more details of further segmentation and image processing methods are
524 described in Mathews & Du Plessis [17], including a step by step guide for segmentation of frog
525 bones from whole frog scans.

526
527 During image processing, filters are initially used to smooth the images and in doing so, to reduce
528 random noise. This is especially useful for noisy data or fast scans, but sometimes this step can
529 smooth over fine structural details, therefore its use is dependent on the image quality and aim of
530 the analysis. Examples of such filters, are Gaussian or Median smoothing.

531
532 Segmentation usually follows the smoothing step, where the respective voxels or regions are
533 grouped together, creating individual regions-of-interest (ROIs) or image masks. In some cases
534 this could include a binarisation step, where the selected voxels are given a value of 1 and the rest
535 a value of 0 (or black and white). Thresholding itself can be done in different ways, and the
536 available methods depend on the software used and algorithms available. One valuable method is
537 local adaptive thresholding, whereby a global threshold or region of interest is chosen as starting
538 contour and local thresholding is then applied. In addition to thresholding and region growing, a
539 very useful method especially for biological sample segmentation is manual segmentation using a
540 drawing tool, to add or remove regions with a virtual pen or brush. This method is a tedious
541 process as it can involve colouring in regions in every slice in the CT data set, but is sometimes
542 the best way to segment complex biological data sets. This process can be accelerated by making
543 use of thresholding or other semi-automated segmentation tools and then refining these selections
544 using the drawing tool (instead of making the entire selection only with the drawing tool). Another
545 possibility is to significantly filter the data, which simplifies the automated segmentation tools, but
546 can result in loss of quality for small features. This is useful when viewing only is required, and not
547 complex dimensional or volumetric measurements are required.

548
549 The next step usually involves image analysis. Image analysis aims to achieve the extraction of
550 qualitative as well as quantitative data from the images or image sequences [5]. The information
551 from the range of 2D slices that are merged to create the 3D image allow for volumetric
552 observations and measurements of the microstructure of the sample. Some typical tools available

553 for micro-CT image analysis are: morphology analysis typically used for bone structure (e.g. mean
554 trabecular number, trabecular spacing, volume fractions), defect detection (detection and size
555 distribution analysis of pores/voids/cracks/inclusions); nominal/actual comparison (compare
556 geometries of two voxel data sets based on their surface information); wall thickness analysis
557 (measure thickness variations of walls of objects or layers of a material) and orientation analysis
558 (orientation of fibers or longitudinal features in 3D) [3]. For more details of reconstruction and
559 image processing post-scan, a recent article describes various options in more detail [18].

560
561 Analyses vary considerably depending on the application, especially in terms of time required. For
562 some general industrial applications, specialised software modules exist to simplify the process of
563 such analyses and minimise the human error involved in the process. Such routine analyses are
564 therefore not very time consuming (usually less than 1 hour for each type of analysis, sometimes
565 much less depending on complexity of data set). Biological data sets in general tend to be more
566 complex and require more time consuming and sometimes custom procedures to be applied. For
567 viewing of segmented features, as shown above both slice images as well as 3D renderings can
568 be used to allow the visualisation of selected features, for example to view connectivity or location
569 relative to other features. Dimensional measurements can be performed in 2D slice views (linear
570 distance measurements) or in 3D using volume or surface area measurements.

571 572 *3.6 Further scanning at higher resolutions*

573 In many cases once an analysis has been completed, it might be realised that more scanning can
574 provide further details, especially with regards to higher resolution scanning of selected regions.
575 One further step is therefore to scan a region at a higher resolution to get a more detailed view.
576 The fact that the same sample can be scanned at varying resolutions can be confusing to the first-
577 time user, especially when also considering varying image quality and scan time possibilities. As
578 an example of the application of the guidelines described in the previous scanning setup section: a
579 20 mm wide sample can be scanned at best at 20 µm resolution with very good quality scan
580 parameters in 40 min (considering 500 ms per image, average 2 images per step position, and
581 2000 images per one full rotation, plus rotational movement time), assuming no errors and not
582 considering setup time or reconstruction time after the scan. Therefore, in total 1 h per scan is
583 generally used for the micro-CT scanner. Longer scan times are possible with increased image
584 quality, but much faster scans are also possible. What can be confusing is the fact that the same
585 quality scan settings can be used as above for the 20 mm wide sample, at 50 µm resolution. In
586 this case less images are required at 50 µm since less pixels of the detector are covered by the
587 sample. In this case the scan time is roughly halved for the same signal-to-noise ratio (or
588 improving further the signal-to-noise ratio for the same scan time by averaging more). From this it
589 can be understood that the scan time becomes shorter as resolution gets poorer, but increases
590 with an improved resolution when the same sample size is used. Once the best resolution for a

592 sample is achieved, the next step for higher resolution is to section the sample, or do a ROI scan
593 of a section which will be described in the next section.

594
595 Other possibilities for further steps include correlation of CT and other analytical techniques, for
596 example correlation between scanning electron microscopy and CT can hold some advantages,
597 where scanning electron microscopy (SEM) shows detailed surface information, CT can extend
598 this with internal connectivity information, for example of porous materials. Another possibility for a
599 further step is to apply some process to the sample, and repeat the scan producing two or more
600 CT data sets to monitor degradation or changes in internal features in a time lapse (termed 4D
601 imaging).

602 603 *3.7 Maintenance issues and usage schedules*

604 Commercial X-ray micro-CT systems all require significant maintenance, which must be
605 considered in terms of financial implications. Although benchtop systems require less maintenance
606 than cabinet and walk-in systems, annual services and replacement parts can still be roughly 10%
607 or more (depending on the usage) of the purchase price of the system. For this reason, the
608 availability of local technical support from a supplier is a major consideration, along with the
609 system type. In general, the larger the system the more maintenance is required.

610
611 In a multi-user facility where the systems are operational for long periods, streamlining the
612 workflow and getting more scans done semi-automated is of interest. For this purpose, some
613 suppliers offer automated sample loading (e.g. 12 samples pre-loaded in a rotating sample
614 mount), automated choice of scan settings and even sending of emails or phone messages when
615 a scan is completed (or failed). Automated batch reconstruction, as well as batch image
616 processing and analysis is possible on multiple scan data sets done overnight when using macros
617 written by the user. This only works for very simple procedures since no human interaction is
618 involved to check the result, but can be time saving for large numbers of data sets. In practice,
619 however, the most widely used method of getting optimal samples done in the available time span,
620 is to load samples vertically and then scan each one sequentially with a vertical-adjusted multiple
621 scan. In this way, approximately 3-10 samples can be scanned overnight, depending on the scan
622 parameters and assuming no hardware failures occurs during the scan time.

623
624 Another misconception regarding micro-CT scanning is the frequency of hardware failures.
625 Especially during continuous-rotation scans, any failure (even only of one image) causes the entire
626 scan to fail. Stepwise rotation limits this problem as the scan is stopped until the system is stable
627 again. However, typical usage for a large cabinet based system requires approximately 10-20 %
628 downtime for repairs and maintenance, as well as consumable replacements (especially filaments)

629 that are required approximately once a week on average. These are all issues and costs not
630 disclosed by CT companies before a purchase.

631 632 3.8 Micro-CT scanning of a three-horned chameleon – an example of data acquisition and analysis

633 The flow diagram depicted in Fig. 6 summarises the considerations, guidelines and options related
634 to micro-CT scanning of biological samples and is suggested to be used as guiding principles
635 when conducting micro-CT scans and analysis. The X-ray micro-CT data acquisition and analysis
636 of the three-horned chameleon, shown as an example, will follow the step-wise guide as presented
637 in Fig. 6.

638
639 Insert Figure 6 approximately here

640
641

641 3.8.1. CT set-up parameters:

- 642 i. The chameleon (wet with alcohol from the collection jar) was mounted on florist foam on
643 top of a cardboard tube (Fig. 7a), after being dried out at ambient conditions for a few
644 hours in this position. The chameleon is seen with its densest and thickest features as
645 darker regions by looking at a digital X-ray projection image of the specimen (Fig. 7b).
- 646 ii. The chameleon's size was adequate for scanning in a cabinet system (total field of view
647 approximately 100 mm wide x 100 mm high), but would also have been possible in a
648 benchtop instrument.
- 649 iii. This example had 2000 pixels in total sample height, and using *Guideline I*, the best
650 possible resolution was obtained at 75 μm . Following *Guideline II*, since the best possible
651 magnification was at 75 μm voxel size, 3200 step positions were used. Since the sample
652 was loaded at 45 degrees, there was a slight improvement in the best possible voxel size
653 compared to horizontal or vertical mounting, for a single scan volume (vertical or horizontal
654 would be limited to longest axis of the chameleon sample).
- 655 iv. Averaging was set to 2 and skipping of the first image at each new position was used.
- 656 v. As the chameleon is a biological sample, no beam filtration was required.
- 657 vi. Initially, a typical image acquisition time of 500 ms was set, with 100 kV and 100 μA as
658 starting point, with no beam filtration. This setting showed a good penetration value, but not
659 very high signal values on the detector, so the current was increased to 200 μA to obtain
660 approximately 8000 counts, where 10 000 is the saturation level of the detector (*Guidelines*
661 *III & IV*). In this process a compromise between scan time and image quality was found.
662 Higher quality would have been possible with more averaging, resulting in longer scan
663 times. Higher quality would also have been possible at lower voltage since the penetration
664 values were quite high. When lowering the voltage, the total X-ray emission from the
665 source reduces, which requires a longer image acquisition time to make full use of the best

possible contrast capable with the detector. This also increases scan time and additionally, lower voltages can cause unexpected artifacts as explained above.

Insert Figure 7 approximately here

3.8.2. Scanning:

- i. Corrected the background;
- ii. Ran a beam centering; and
- iii. Loaded the sample that was mounted on florist foam and started the image acquisition process.
- iv. Monitor the process to correct for any errors

3.8.3. Reconstruction settings used for the chameleon scan included:

- i. cropping to remove unwanted regions around the edges;
- ii. 16 bit data type selected;
- iii. offset correction by using a scan optimisation process;
- iv. a low beam hardening correction value; and
- v. a background intensity value used to correct for variations in intensity.

3.8.4. The 3D visualisation of the chameleon is shown in Fig. 8 with:

- i. a simple thresholding function allowing the visualisation of the skeleton structure which is denser than the rest of the animal;
- ii. the data set was processed to virtually remove the mounting material; and
- iii. smoothed to produce a clean surface rendering.

Image processing steps are described in more detail in the next section.

Insert Figure 8 approximately here

3.8.5. Image processing and analysis:

As one example, an interesting bony feature is highlighted in red in Fig. 9, this structure is a part of the very strong tongue of the animal (due to its use for catching prey). A slice image shows more detail and is shown here in the plane of the bony feature, indicating that this bony feature is extremely straight. It is possible to view this in 3D rendering as well by making the rest of the animal semi-transparent and the feature of interest non-transparent. An example of image analysis would be to measure the length and width of the bony feature of the tongue of the chameleon, as well as determine its surface area and volume.

Insert Figure 9 approximately here

704
705
706
707
708
709
710
711
712
713
714
715
716
717
718
719
720
721
722
723
724
725
726
727
728
729
730
731
732
733
734
735
736
737
738
739
740
741
742
743
744
745

3.8.6. Further scanning at higher resolutions:

Since the head of chameleon is quite striking and the horns in particular are interesting to study in more depth, a close-up scan of the head of the animal was made. This is a nice example showing how the same sample can be scanned at different resolutions without sectioning, or in multiple ways to get different types of information. In this ROI scan, the resolution was 30 μm (with a field of view of about 30 mm) compared to the full body scan of 75 μm (field of view 75 mm). The higher resolution allows smaller features to be visualised and segmented (isolated) more easily. Fig. 10a shows the 3D surface view of the head with false colour for visual appearance, Fig 10b shows the skeletal structure in white, and Fig 10c shows a cropped view of the skeleton depicting the central horn's internal microstructure. If the entire animal needs to be scanned at 30 μm , this would be possible using an automated multiple-scan process, whereby a sequence of scans are performed at different height positions across a vertically mounted sample. The multiple scans are then stitched together to form a large data set. This process takes longer and is therefore more costly, and is usually only required in specialised situations.

Insert Figure 10 approximately here

Even though X-ray tomography is generally known as a non-destructive technique, sample preparation for very high resolution scans can be somewhat destructive. This is because of practical limitations of sample size. A good example is the horn of the chameleon, which shows an interesting microstructure visible in Fig.10 at 30 μm resolution. If this microstructure needs further and more detailed investigation, scanning it at higher resolution may be necessary. Higher resolution involves moving the sample closer to the X-ray source, but the sample must still be able to make a full rotation, which is practically not possible when doing a 10 μm scan of the horn. The horn was in this example sectioned and removed from the chameleon, and mounted in florist foam on top of a glass rod (Fig. 2c). The 10 μm scan was done in a nano-CT instrument rather than the micro-CT. The reason for this is that although both systems overlap in their abilities to scan objects from 5 – 30 μm , typically any sample smaller than 5-10 mm wide, produces better image quality from the nano-CT instrument. The improvement comes mainly from the stabilisation of the air-bearing rotation stage, but in general the system is best suited for high resolution objects and produces sharper images for fine structures. It is similar to most benchtop micro-CT systems, which is well known to biologists in general due to their wide availability. The result of this horn-only scan is shown in Fig. 11 in a side-slice image. This clearly shows an increased image quality and resolution allowing a detailed analysis of the microstructure of the entire horn. Such analysis is not attempted in the scope of this paper, but the data is included for interested researchers to make use of.

742 Insert Figure 11 approximately here

743
744 Although Fig. 11 shows the horn's internal bony microstructure in great detail, an even higher
745 resolution scan of the tip of this structure was done at 4 μm as a demonstration of the capabilities
746 of the technique, and in such a way that the width of the sample fits the detector. The resulting CT
747 slice image in Fig. 12a shows great detail with some indication of black spots in the dense bony
748 structure, indicating the presence of osteocytes. The structure is visualised in 3D as well in Fig.
749 12b.

750
751 Insert Figure 12 approximately here

752
753 Since the detail of Fig. 12a shows signs of osteocytes within the bony structure, a sub-micron scan
754 was attempted of this material. This required further sectioning, to allow a full field of view of
755 approximately 1.5 mm only. The resulting scan at 950 nm (0.95 μm) is shown in Fig. 13a in a 2D
756 slice image which clearly resolves the osteocytes and in Fig. 13b showing the osteocytes in 3D
757 with a colour-coded volume analysis. This sequence of scans indicates the capabilities of multiple
758 resolution scanning, providing different types of information and allowing different types of image
759 analysis. Data sets are included and researchers are urged to make use of these.

760
761 Insert Figure 13 approximately here

762 4. Summary

763 3D laboratory X-ray micro-CT is a fast growing non-destructive testing and analysis method in
764 scientific research applications. The increasing accessibility of such instruments will lead to an
765 increasing number of new discoveries in scientific research applications in biological sciences in
766 particular. The aim of this paper was to provide a focused "how-to" guide for new potential users to
767 better plan their work, and understand how to best make use of this technology. A specific new
768 case study was used as demonstration – the Jackson's three-horned chameleon specimen which
769 was scanned at different settings, and the full data sets provided as supplementary information.
770 These data sets are meant to be used to gain a better understanding for viewing and handling
771 typical 3D data sets from the technique. An interesting feature related to the tongue of the animal
772 was segmented in 3D and found to be extremely straight, and the skeletal structure was
773 demonstrated by simple thresholding. Scans up to submicron resolution resolved osteocyte
774 structure in the horn of the chameleon. These observations demonstrate a typical multiscale
775 investigation by X-ray micro- and nano-CT, which usually lead to exciting new observations in
776 three dimensions.

778 **5. Acknowledgements**

779 The Botany and Zoology Department at Stellenbosch University is thanked for lending the
780 chameleon specimen used in this study.
4
5

781 **6. References**

8
782 1. Kalender WA. X-ray computed tomography. *Physics in Medicine and Biology*. 2006;51(13):29-
10 43
11
1284 2. Brunke O. High-resolution CT-based defect analysis and dimensional measurement. *Insight-
13 Non-Destructive Testing and Condition Monitoring*. 2010;52(2):91-3
1485
15 3. Singhal A, Grande JC, Zhou Z. Micro/Nano CT for visualization of internal structures.
16 *Microscopy Today*. 2013;21(02):16-22
1787
18 4. Mizutani R, Suzuki Y. X-ray microtomography in biology. *Micron*. 2012;43(2):104-15
1888
20 5. Schoeman L, Williams P, du Plessis A, Manley M. X-ray micro-computed tomography (μ CT) for
21 non-destructive characterisation of food microstructure. *Trends in Food Science & Technology*.
2290
23 2016;47:10-24
2491
25 6. Cnudde V, Boone MN. High-resolution X-ray computed tomography in geosciences: A review of
26 the current technology and applications. *Earth-Science Reviews*. 2013;123:1-17
2793
28 7. Maire E, Withers PJ. Quantitative X-ray tomography. *International Materials Reviews*.
2994
30 2014;59(1):1-43
3195
32 8. Landis EN, Keane DT. X-ray microtomography. *Materials characterization*. 2010;61(12):1305-16
33
3497 9. Stauber M, Müller R. Micro-computed tomography: a method for the non-destructive evaluation
35 of the three-dimensional structure of biological specimens. *Osteoporosis: Methods and Protocols*.
3698
37 2008:273-92
38
3900 10. Kotwaliwale N, Singh K, Kalne A, Jha SN, Seth N, Kar A. X-ray imaging methods for internal
40 quality evaluation of agricultural produce. *Journal of Food Science and Technology*. 2011;51(1):1-
4101
42 15
43
4403 11. Duluiu OG. Computer axial tomography in geosciences: an overview. *Earth-Science Reviews*.
45 1999;48(4):265-81
4604
47 12. Kak AC, Slaney M. *Principles of computerized tomographic imaging* New York: IEEE Press;
48 1988.
4906
50 13. Lin C, Miller J. Cone beam X-ray microtomography-a new facility for three-dimensional
5107
52 analysis of multiphase materials. *Minerals and Metallurgical Processing*. 2002;19(2):65-71
5308
5409 14. Hanke R, Fuchs T, Uhlmann N. X-ray based methods for non-destructive testing and material
55 characterization. *Nuclear Instruments and Methods in Physics Research Section A: Accelerators,
5610
57 Spectrometers, Detectors and Associated Equipment*. 2008;591(1):14-8
5811
5912 15. Feldkamp L, Davis L, Kress J. Practical cone-beam algorithm. *JOSA A*. 1984;1(6):612-9
60
61
62
63
64
65

- 813 16. Donis-González IR, Guyer DE, Pease A, Barthel F. Internal characterisation of fresh
1
814 agricultural products using traditional and ultrafast electron beam X-ray computed tomography
2
815 imaging. *Biosystems Engineering*. 2014;117:104-13
4
816 17. Matthews T, Du Plessis A. Using X-ray computed tomography analysis tools to compare the
6
817 skeletal element morphology of fossil and modern frog (Anura) species. *Palaeontologia
7
818 Electronica* 2016;19(1): 1-46
9
819 18. Liu Y, Kiss AM, Larsson DH, Yang F, Pianetta P. To get the most out of high resolution X-ray
11
820 tomography: A review of the post-reconstruction analysis. *Spectrochimica Acta Part B: Atomic
12
821 Spectroscopy*. 2016;(117):29-41
14
1522
1623
17
18
19
20
21
22
23
24
25
26
27
28
29
30
31
32
33
34
35
36
37
38
39
40
41
42
43
44
45
46
47
48
49
50
51
52
53
54
55
56
57
58
59
60
61
62
63
64
65

824 **Tables:**

1
825 **Table 1.** Summary of faulty or problematic CT scans as discussed throughout this paper, stating
826 problems, causes and possible solutions, respectively.
4

827

6

7

8

9

10

11

12

13

14

15

16

17

18

19

20

21

22

23

24

25

26

27

28

29

30

31

32

33

34

35

36

37

38

39

40

41

42

43

44

45

46

47

48

49

50

51

52

53

54

55

56

57

58

59

60

61

62

63

64

65

Problem	Cause	Solution
Grainy image	Image acquisition time too low	Increase image acquisition time
Streaky artifacts	Differences in absorption from different angles; X-ray penetration is insufficient	Increase voltage
Poor contrast	Too high voltage is used	Reduce voltage
Blurred image	Improper sample mounting; allowing sample to move during scanning	Proper mounting to ensure no movement during scanning
Stitching artifacts / vertical or horizontal line	Sample too wide for a single scan	Make sub-sections of sample; use a smaller sample or less magnification
Beam hardening / cupping effect	Edge of sample seems brighter than the inside of the sample due to insufficient penetration of the sample	Reconstruction: use beam hardening correction option, or scan with higher voltage and more beam filters
Small movement or shift (double edge)	Inaccuracy of rotation stage or movement of sample	Reconstruction: do an offset correction; or rescan if offset cannot be corrected. Reset stages. Hardware could be faulty, e.g. tilt axis alignment
The histogram is shifted strongly to one side	Small quantity of bright dense phase are present, but irrelevant	Reconstruction: make use of the clamping option
Scattering	Causes brighter or darker projection images from different angles	Reconstruction: select background detector counts in each image and normalise across the series of images
Ring artifacts	Bright rings are visible in the top slice view	Reconstruction: make use of ring artifact reduction by disregarding 'dead' pixels from the projection image (or disregard pixels in the acquisition process)

1
2
3
4
5
6
7
8
9
10
11
12
13
14
15
16
17
18
19
20
21
22
23
24
25
26
27
28
29
30
31
32
33
34
35
36
37
38
39
40
41
42
43
44
45
46
47
48
49
50
51
52
53
54
55
56
57
58
59
60
61
62
63
64
65

Central rotation artifact	The center of rotation is visible as a line in a side slice view, or a dot with concentric rings from the top view.	Make use of detector shift option in acquisition, which smooths out the artifact.
Bright ring around outside of scan volume, resulting in poor image quality	In ROI scans where the sample extends over the side of the 2D image	Use special reconstruction algorithm which corrects for this, or crop the ROI further in reconstruction
Cone beam artifacts	Affecting the edges of materials near the edges of the detector	Use less magnification to fill less pixels on detector

834 **Figure captions:**

835
836 Figure 1. The fundamental components of a micro-CT instrument.

837
838 Figure 2. Different mounting styles are depicted in (a) where the whole chameleon is wrapped in
839 cloth for wet scanning, (b) the whole chameleon is mounted upright in coke bottle for vertical
840 multiple scanning and (c) a nano-CT sample mount of a 1.5 mm section of the chameleon's horn.

841
842 Figure 3. A graph of the typical resolution obtained when working with different sample sizes.

843
844 Figure 4. Micro-CT slice images of the chameleon, where (a) a metal tag is included in the scan
845 volume, resulting in streaky artifacts, (b) too low voltage was used and therefore image artifacts
846 are found around dense parts of chameleon and (c) too high voltage was used, showing poor
847 contrast.

848
849 Figure 5. Micro-CT slice images of the chameleon, showing poor images caused by (a)
850 reconstruction clamping set too high, resulting in poor contrast, (b) double edges due to incorrect
851 offset calculations during reconstruction, and (c) slight blur due to tilt-axis misalignment.

852
853 Figure 6. A step-wise guide for micro-CT scanning and data analysis, featuring settings,
854 considerations, guidelines and options related to micro-CT imaging and analysis of biological
855 sample.

856
857 Figure 7. Images demonstrating the mounting of the three-horned chameleon with (a) showing the
858 florist foam mounting material that forms the basis on which the specimen is placed, and (b) the X-
859 ray projection image showing the very low density of the mounting material.

860
861 Figure 8. 3D reconstructions of the three-horned chameleon with a (a) surface view and (b) a
862 semi-transparent view showing the dense skeleton structure in yellow.

863
864 Figure 9. (a) An isolated bony feature related to the tongue of the animal is shown in red in a 3D
865 view, with (b) showing this feature in a CT slice image.

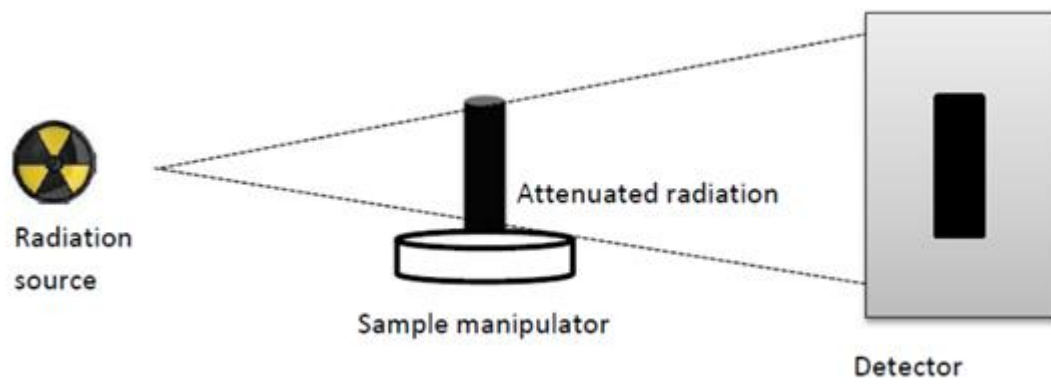
866
867 Figure 10. A high resolution ROI scan (30 μm) of the head of the three-horned chameleon with (a)
868 a 3D surface view, (b) a skeleton view and (c) a cropped skeleton view.

869
870 Figure 11. Nano-CT slice image of the horn of the chameleon at 10 μm , illustrating sectioning.

872 Figure 12. (a) Nano-CT slice image showing in great detail (4 μm) the dense structure of the bone
1
873 inside the chameleon horn, with (b) visualizing the bone structure in 3D.
2

874
4
875 Figure 13. (a) Nano-CT scan revealing osteocyte distribution in the tip of the chameleon horn's
6
876 internal bony microstructure at sub-micron resolution of 0.95 μm , with (b) showing the osteocytes
7
877 in 3D along with a colour-coded volume analysis.
9

10
11
12
13
14
15
16
17
18
19
20
21
22
23
24
25
26
27
28
29
30
31
32
33
34
35
36
37
38
39
40
41
42
43
44
45
46
47
48
49
50
51
52
53
54
55
56
57
58
59
60
61
62
63
64
65



(a)

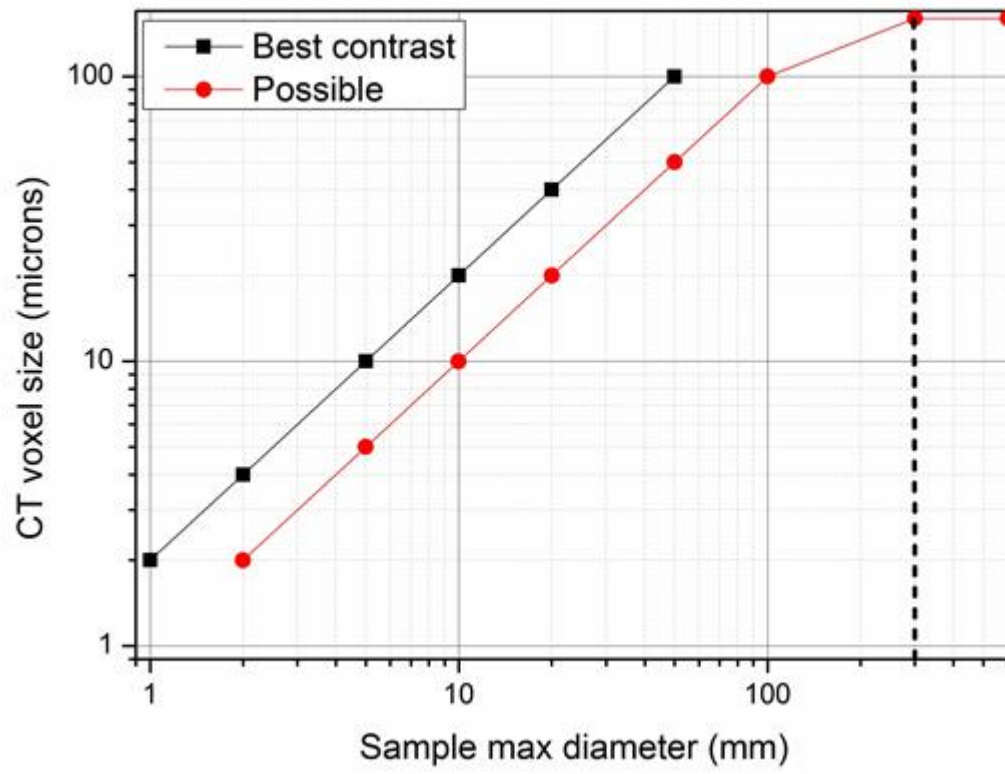


(b)



(c)

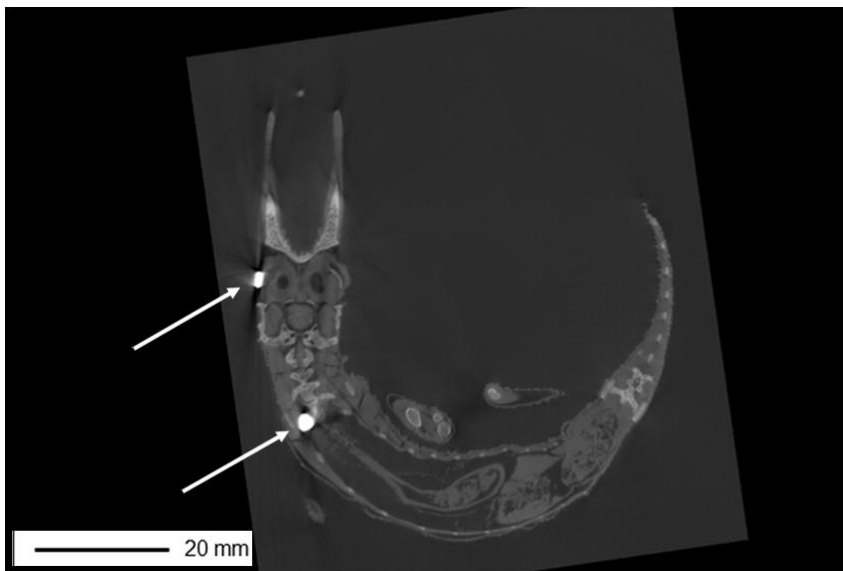




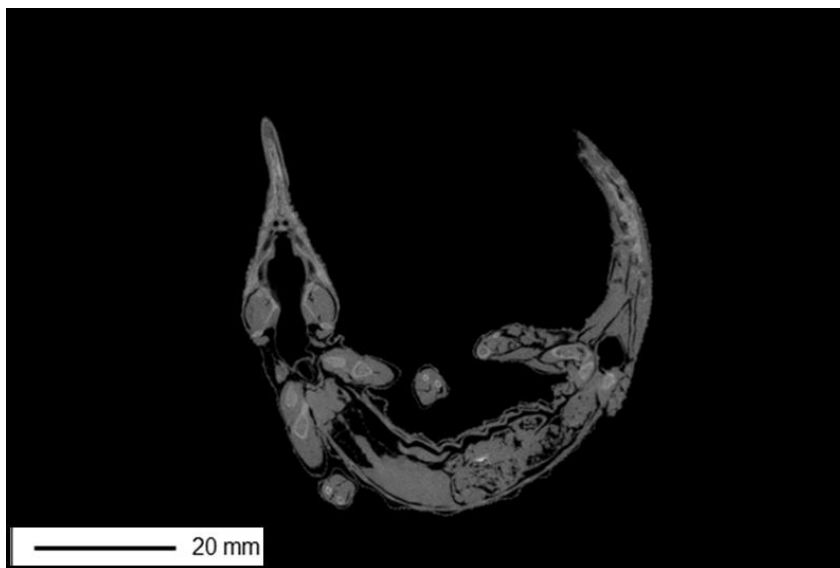
(a)



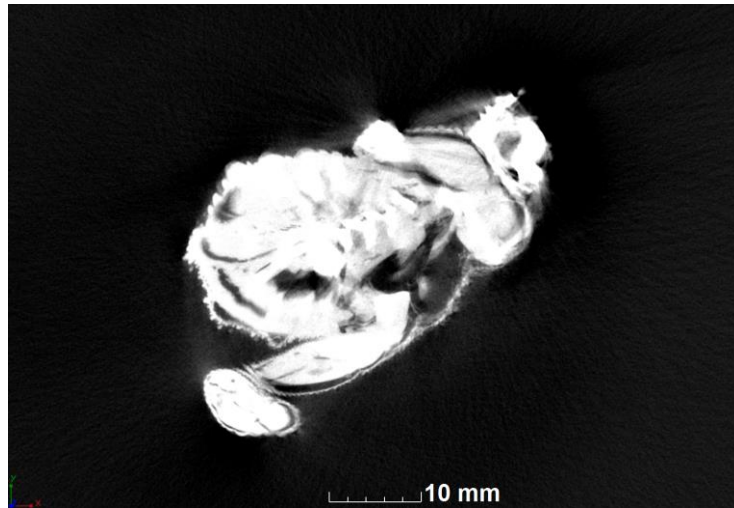
(b)



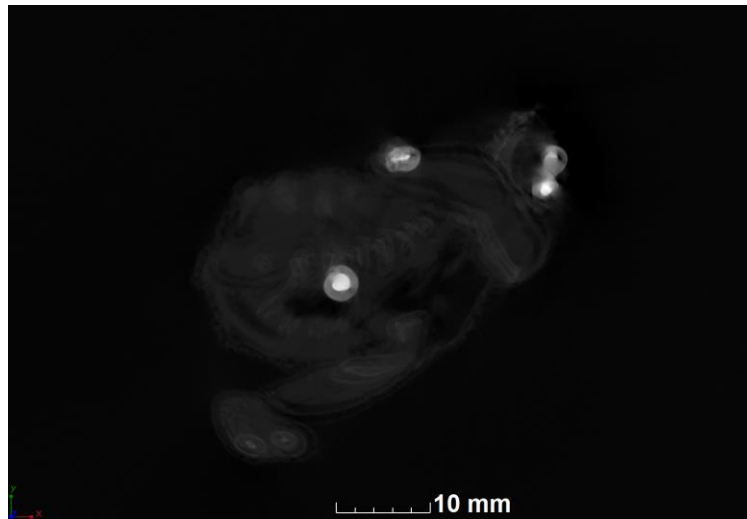
(c)



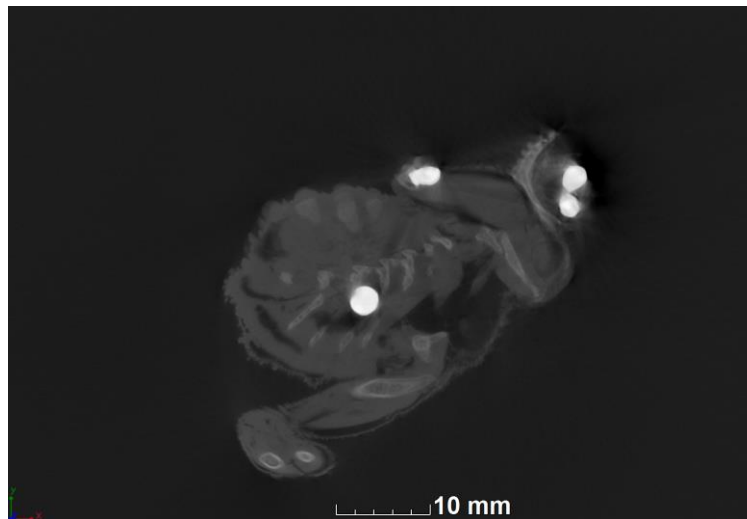
(a)



(b)



(c)



1. CT Set-up parameters

- Sample preparation and mounting (Figure 7)
- Considering size for correct resolution setting: *Guideline I*
- Choosing step positions and averaging: *Guideline II*
- Choosing voltage settings: *Guideline III*
- Choice of filtration of beam and detector
- Calculating penetration ratio: *Guideline IV*

2. Scanning

- Normalising / correcting the back ground
- Run a beam centering
- Load sample and commence scanning
- Monitor the process

3. Reconstruction

- Cropping the field of view
- Choice of data type
- Offset correction
- Beam hardening correction
- Correct for variation in intensity - normalisation step

4. Visualisation (Figure 8)

- Thresholding function
- Removal of mounting material
- Smoothing
- Surface rendering

5. Image processing and analysis

- Segmentation: Thresholding, region growing, drawing tool (Figure 9)
- Smoothing using filters
- Image analysis: length & width measurements, surface area analysis, volume analysis

6. Further scanning at higher resolution

- Close-up scans:
 - head: 30 μm ROI scan (Figure 10)
 - horn: 10 μm sectioning scan (Figure 11)
 - tip of horn: 4 μm sectioning scan (Figure 12)
 - tip of horn: 0.95 μm sectioning scan (Figure 13)

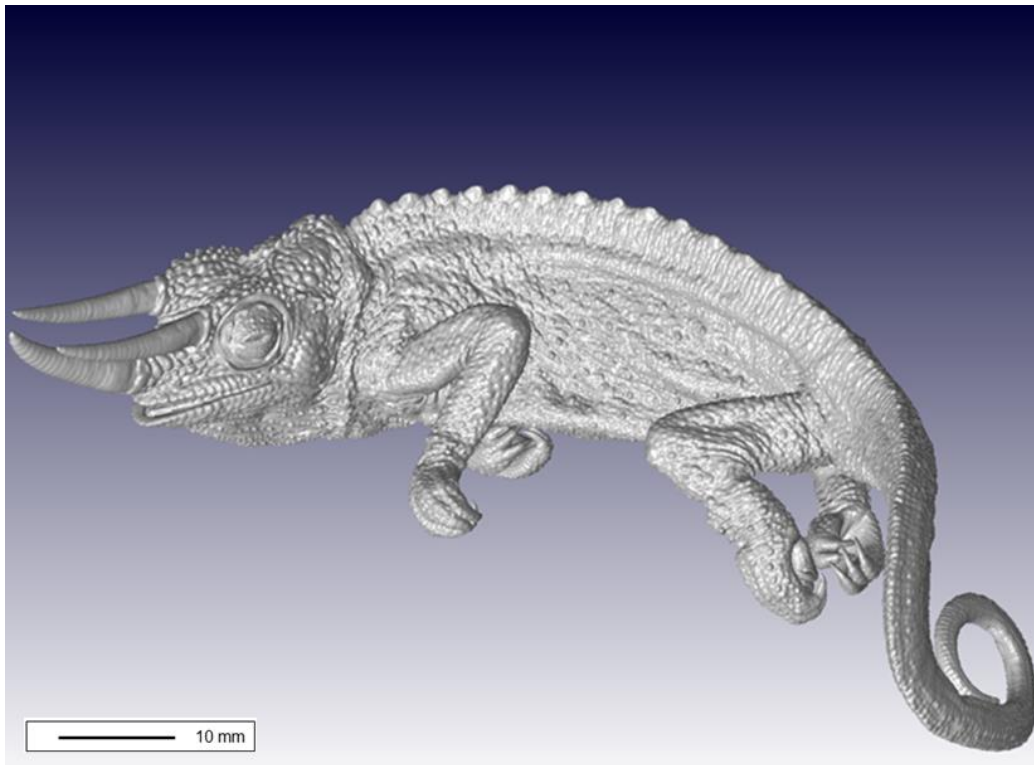
(a)



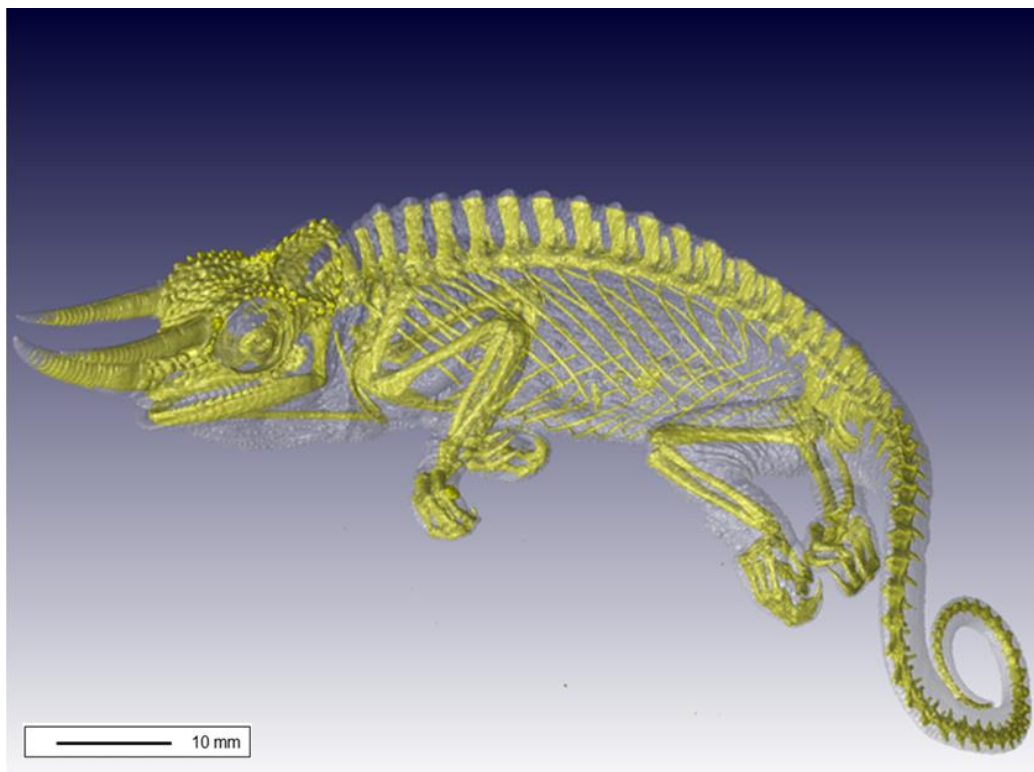
(b)



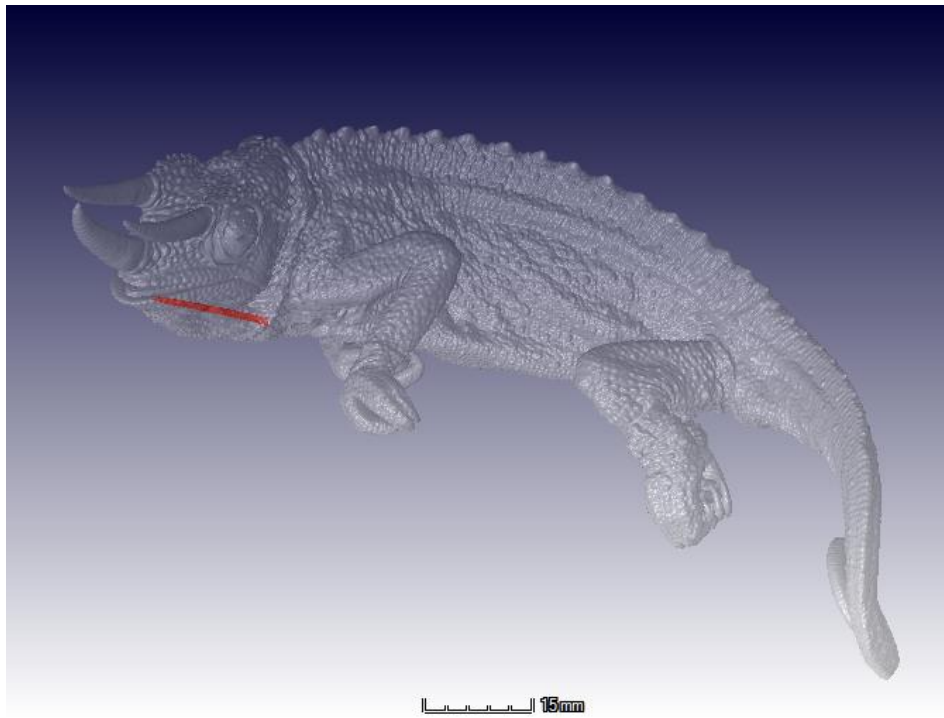
(a)



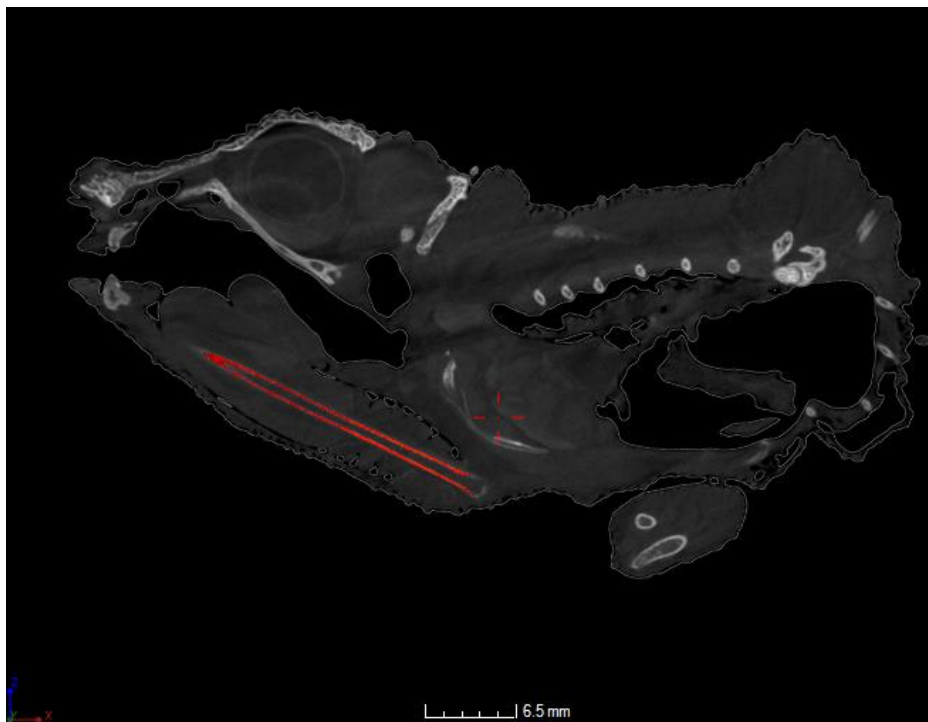
(b)



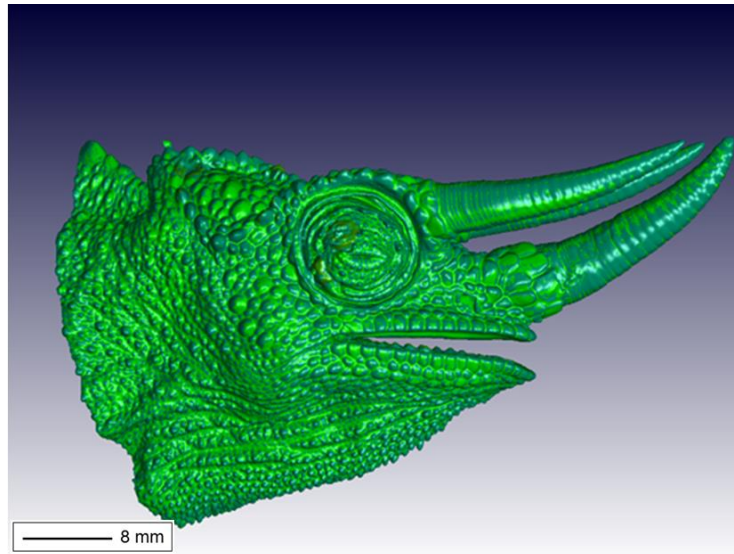
(a)



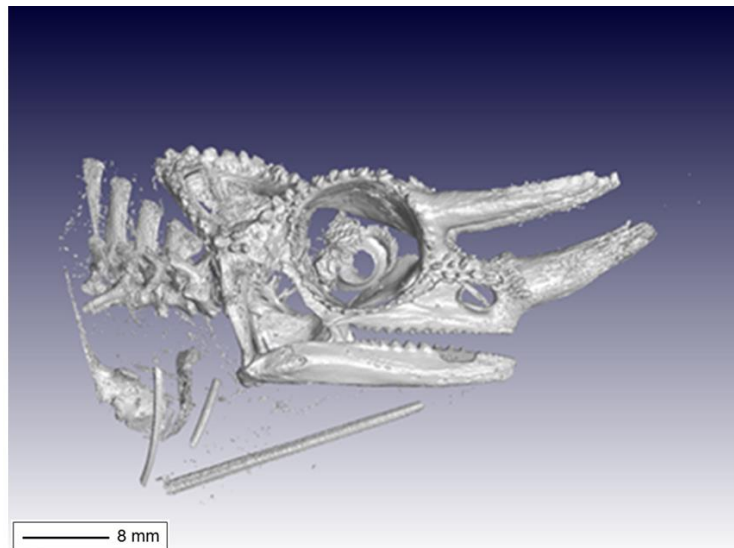
(b)



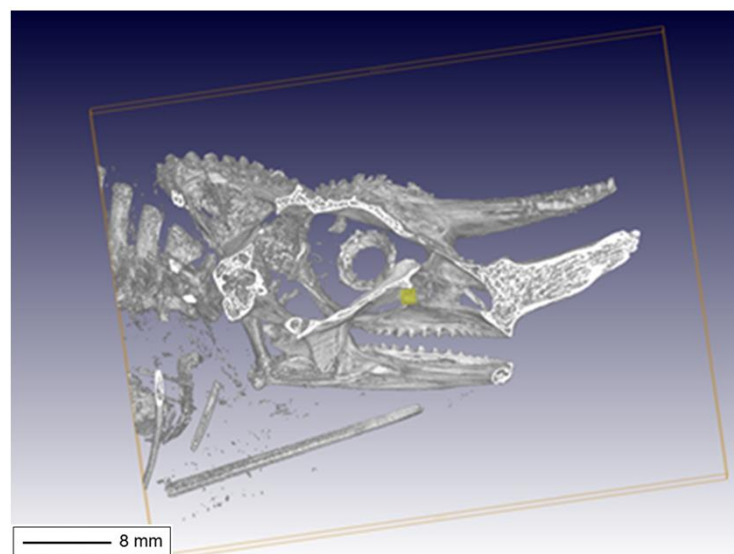
(a)

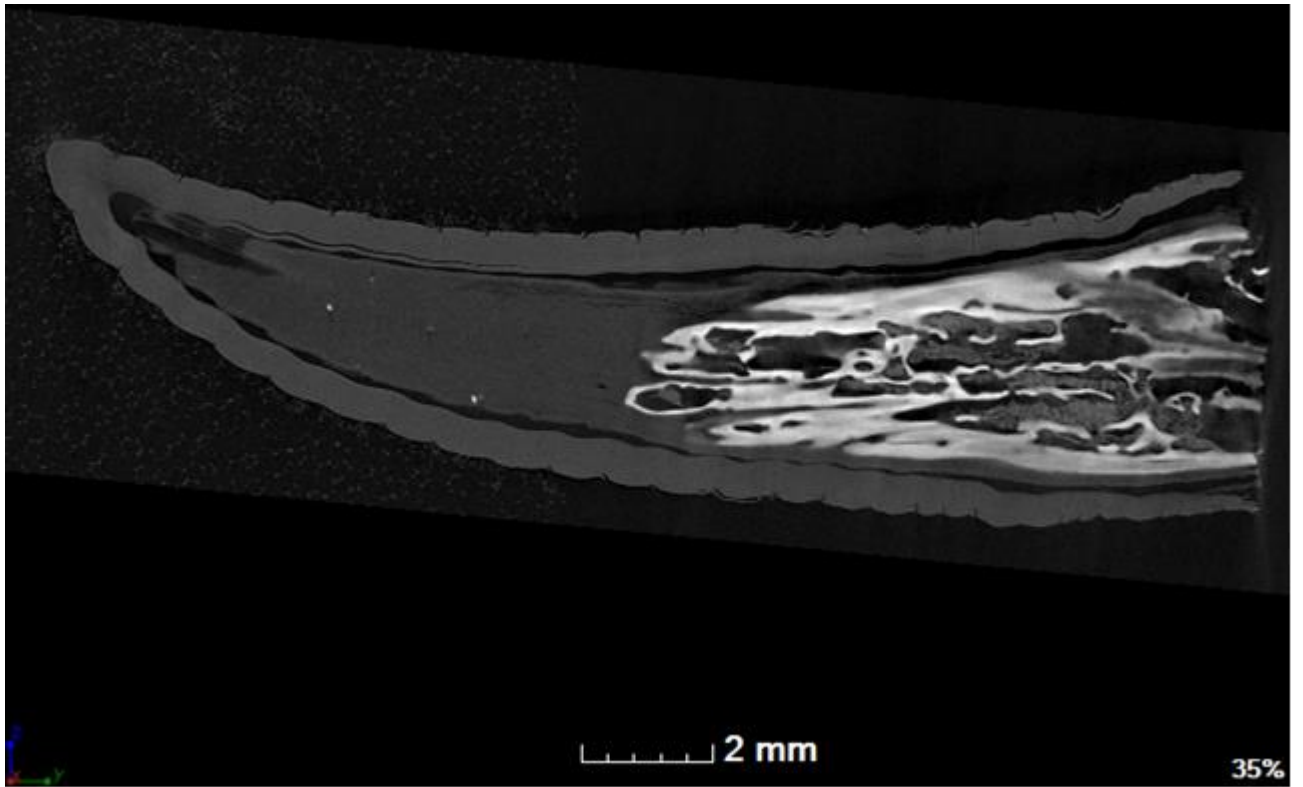


(b)

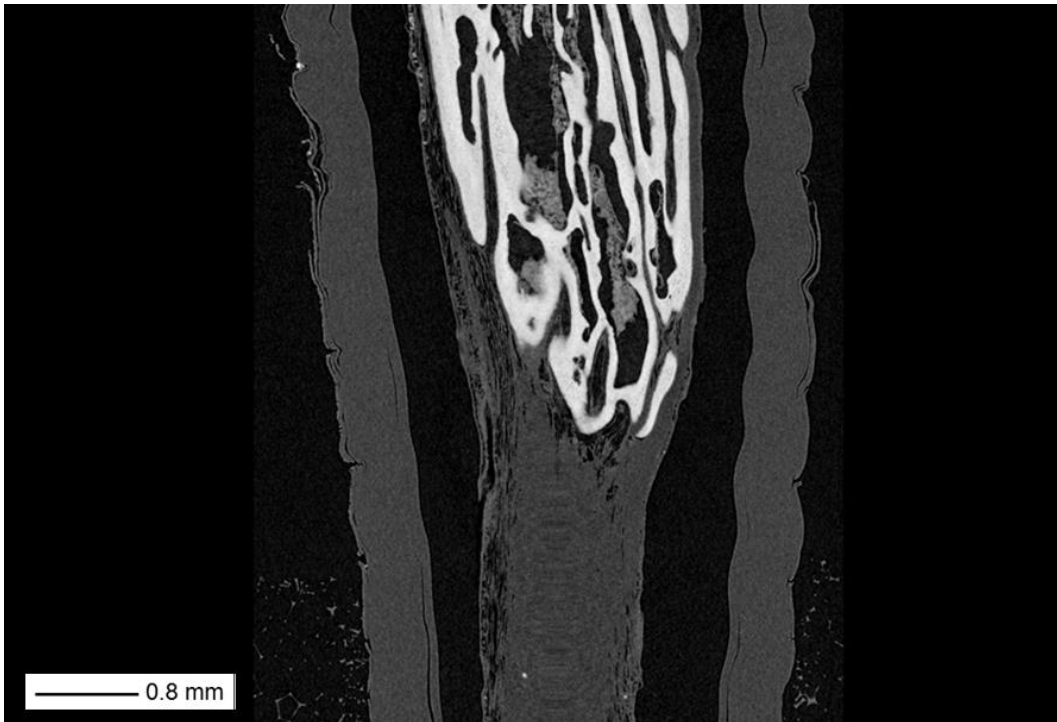


(c)

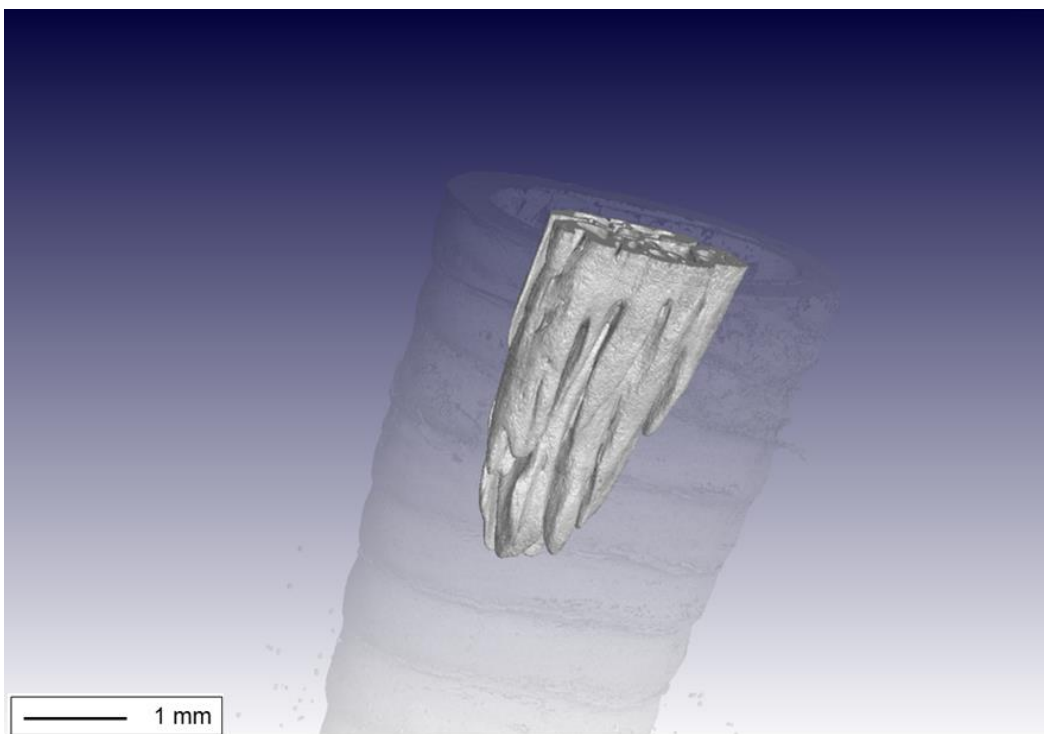




(a)



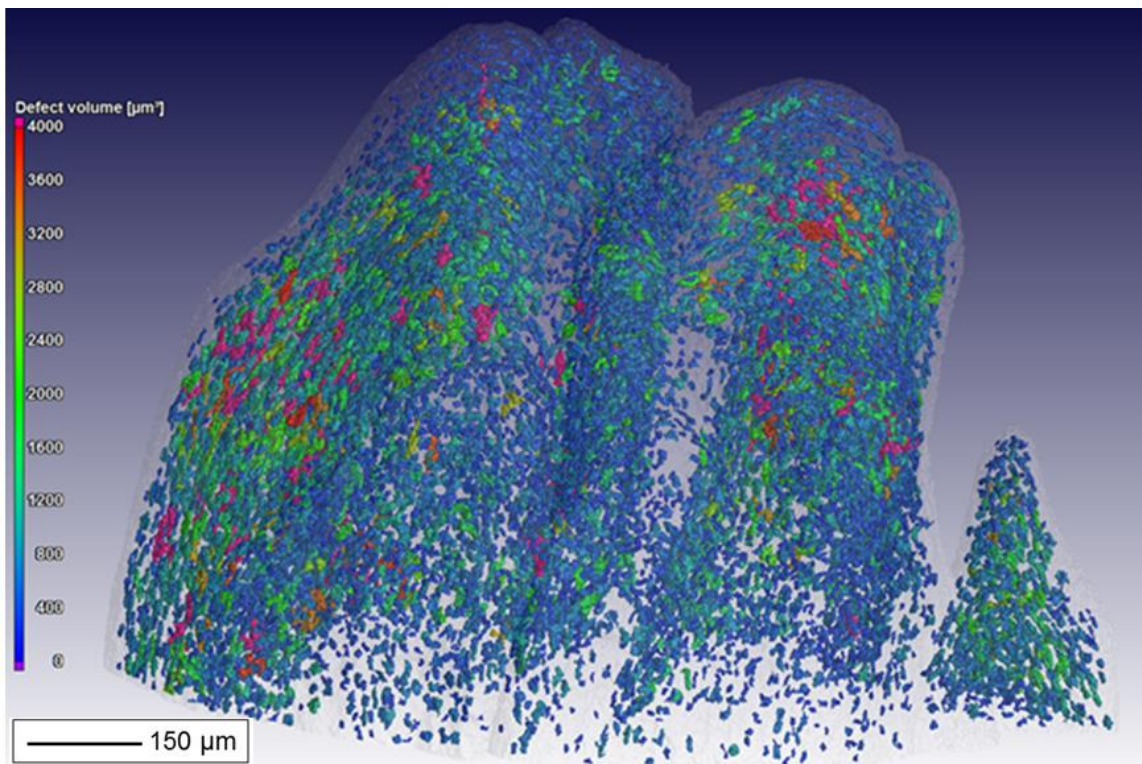
(b)



(a)



(b)



7 June 2016

Dr Scott Edmunds

Editor

GigaScience

Dear Dr Edmunds

Re: Resubmission of manuscript GIGA-D-16-00019 for GigaScience

We hereby re-submit our manuscript titled: **Laboratory X-ray micro-computed tomography: a generalised approach for biological samples using a three-horned chameleon as example** (previous title: X-ray microtomography at Stellenbosch University: a new users guide). This new submission has been considerably reworked thanks to valuable comments from the reviewers. We added an author who assisted significantly in the rework process.

We restructured the manuscript to remove all reference to our facility and specific manufacturers in order to generalise the guidelines provided. We used the chameleon as example to walk the reader through the entire process, demonstrating the application of guidelines provided. Our focus was on providing solutions to possible problems and included examples to demonstrate some of these. We hope this now caters for non-experts and experienced users alike. We also added new data sets of higher resolution scans of the horn of the chameleon to demonstrate the capabilities of multi-scale CT and nano-CT. More details of changes made during the rework process is described point-by-point in response to reviewer comments below.

Reviewer #1:

1. The authors removed any information specific to the Stellenbosch CT facility and focussed on micro-CT facilities in general.

Specifically:

- we added information on exposure time, filters, samples size and material and other factors related (see Sections 3.1.2 to 3.1.6 (pp. 5 – 10) in the revised manuscript). We added examples of good / bad projection images throughout the revised manuscript, adding figures (refer to Figs 4 and 5 in the revised manuscript) and also summarised these examples in a Table (see Table 1 (pp.

- 2 – 25) in revised manuscript), including the causes and problem solving options.
- p.4, line 1 (now p. 7, line 251) was changed to include the words “if available” and now reads “...it is advisable to use the skip function, if available, which ignores the first image acquired at each new step...”
 - All topics covering resolution, sample size, detector size etc. were changed to supply general descriptions that can be useful to any user at any facility (see Section 3.1 (pp. 4 – 10) in the revised manuscript).
 - P. 5, line 30 has been changed and now covers two sub-sections (see Section 3.1.3 (pp. 6 – 7, lines 211 – 231) and Section 3.1.5 (pp. 8 – 10, lines 268 – 334), in particular lines 305 – 308 in the revised manuscript) with more general explanations and guidelines. With regards to the comments about the filters and their placement, please see Section 3.1.5 p. 9, lines 310 – 319 in the revised manuscript that addresses this.
 - P. 5, line 47 and following has been changed and now covers a section dedicated to the relationship between voltage and current. Please see Section 3.1.5 (pp. 8 – 10, lines 268 – 335) in the revised manuscript.
 - P. 6, paragraph 2.3 has been rewritten and is now presented as Section 3.1.1 (pp. 4 – 5) with additional figures (Figs. 2a, b and c) in the revised manuscript, covering aspects of mounting. Artifacts related to sample mounting is presented in Table 1 (pp. 23 -24), although other artifacts are covered in Section 3.1.6 (p.10, lines 337 – 359) in the revised manuscript.
 - P. 6, paragraph 2.4 was revised in that any information relating to the Stellenbosch facility was removed, and a new section was added (see Section 3.3.2 Data output styles (pp. 13 – 14, lines 463 – 495) in the revised manuscript), covering different output types.
 - P. 6, paragraph 2.5 was changed in order not to convey any lab-specific information, but rather incorporate a list of commonly used software packages. Please refer to Section 3.4 Visualisation (p. 14, lines 497 – 508) in the revised manuscript. It was also attempted to explain volume rendering, surface modelling, as well as CAD, also giving the full wording for the acronym CAD – please see Section 3.4 Visualisation (p. 14, lines 497 – 508) in the revised manuscript.
 - P. 7, paragraph starting with line 17 has been changed completely and is now presented as Section 3.5 Image processing and analysis (pp. 14 – 16, lines

510 – 570) in the new manuscript. References (Matthews & Du Plessis, Singhal et al., Schoeman et al. and Liu et al.) has been added.

- P. 7, line 39 has been removed.
 - P. 7, section 3 was removed from the manuscript.
 - P. 8, section 4 has been changed following the first approach as suggested by the reviewer. The chameleon example has been used to demonstrate all the relevant steps that needs to be followed when doing micro-CT scanning. A guide has also been presented in the form of a flow diagram. Please refer to [Section 3.8 Micro-CT scanning of a three-horned chameleon – an example of data acquisition and analysis \(pp. 18 – 21, lines 632 – 761\)](#), [Fig. 6 \(flow diagram\)](#) and [figures relating to the scans \(Figs. 7 – 13\)](#) in the revised manuscript. Additional multi-scale X-ray analysis were added of the structure of the chameleon's horn.
 - Section 5 was removed from the manuscript.
 - P.16, line 11 and following was removed from the manuscript.
2. As suggested by the reviewer, schematic illustrations of concepts, illustrations of scanned images showing the effect of various settings and flow diagrams were included in the manuscript.
- These are found as [Fig. 1](#), a schematic illustration of the fundamental components of a micro-CT instrument, [Fig. 2](#) illustrating different mounting styles, [Figs. 4 and 5](#) illustrating examples of poor images and relevant artifacts, and [Fig. 6](#) being a flow diagram or a step-wise guide for micro-CT scanning, applied on the chameleon example. [Fig. 3](#) has also been included in the revised manuscript and is a graph of the typical resolution obtained when working with different sample sizes, thereby explaining a rather complex concept, visually.
 - A comment was raised about figure legends that should describe whether volume or surface rendering was used. As only surface rendering was used in all the images, the authors did not include this into the legends.
 - Everything regarding 3D printing was removed from the manuscript.
3. To address this comment of the reviewer, the authors decided that the paper should be accessible to established as well as new CT users. More detail was thus added on all relevant topics, including scan works, reconstruction, image processing and analysis.
4. Acronyms were all given in full before being abbreviate.

5. The species name was corrected (See p. 4, line 116 in the revised manuscript).

Reviewer #2:

General comments:

- All referencing towards the CT facility at Stellenbosch University was removed.
- The paper was revised to focus on micro-CT facilities in general and also solely on the analysis of biological samples.
- Soft tissue staining was addressed in Section 3.1.1 p. 4, lines 132 – 138 in the revised manuscript.
- Synchrotron CT differences were addressed on p. 2, lines 56 – 61 in the revised manuscript.
- The question relating voxel and spatial resolution was addressed in the newly added Section 3.1.3 pp. 6 – 7, lines 211 - 226 in the revised manuscript.
- A section on artifacts was provided in Section 3.1.6, p. 10, lines 336 – 358, also included in a table, Table 1 and figures, Figs. 4 and 5 in the revised manuscript.
- Detector size was addressed in the newly added section Section 3.1.4, pp. 6 – 7, lines 211 – 232 in the revised manuscript.
- Maintenance issues were addressed in Section 3.7, pp. 17 – 18, lines 603 – 631 in the revised manuscript.
- Overnight scanning were also addressed in Section 3.7, pp. 17 – 18, lines 603 – 631 in the revised manuscript.
- Fast scout scans were addressed on p. 11, lines 376 – 381, as well as p. 15, lines 528 – 530 in the revised manuscript.
- Filters were included in the newly added Section 3.1.5 p. 9, lines 310 – 319 in the revised manuscript.
- Numerous relations with regards to resolution was included in Sections 3.1.2 and 3.1.3 (pp. 5 – 7, lines 211 – 232) in the revised manuscript.
- An overview on mounting techniques were added in Section 3.1.1 Sample preparation and mounting, pp. 4 – 5, lines 130 – 174, including Figs. 2a, b and c in the revised manuscript.
- Sample preparation was addressed in Section 3.1.1 Sample preparation and mounting, pp. 4 – 5, lines 130 – 174, in the revised manuscript.
- Signal-to-noise ratio was further explained in terms of resolution in Section 3.6, pp. 16 - 17, lines 573 – 593 in the revised manuscript.

- Datasets were further explained in [Section 3.3.2, p. 13 – 14, lines 463 – 495](#) in the revised manuscript, covering explanations on data volume.
- Data formats were also covered in the newly added [Section 3.3.2, p. 13 – 14, lines 463 – 495](#), in the revised manuscript.
- The addition of scales to stacks and the calibration thereof has been covered in [Section 3.3.2, p.14, lines 487 – 495](#), in the revised manuscript.
- Open source software packages, amongst others, were included in [Section 3.4, p. 14, lines 497 – 508](#) in the revised manuscript.
- The chameleon example was used for both micro-CT and nano-CT scans and illustrated the differences between the two systems. Please refer to [Section 3.8 Micro-CT scanning of a three-horned chameleon – an example of data acquisition and analysis, pp. 18 – 21, lines 632 – 761](#) in the revised manuscript.
- The differences between 8 and 16-bit files were explained in [Section 3.3.2 Data output types, p.13, lines 463 – 475](#) in the revised manuscript.
- The calibrated status of image stacks has been addressed in [Section 3.3.1, p. 14, lines 487 – 495](#) in the revised manuscript.
- The line that mentions “can take up to 4 weeks” were deleted from the manuscript.
- The reviewer are thanked for introducing the authors to Stauber & Muller. This reference was added to [line 75, p. 3](#).

Specific comments:

- Section 3, as well as Table 1 was removed from the manuscript.
- Sections 5.2, 5.5, 5.6 and 5.10 were removed from the manuscript.
- A figure ([Fig. 7](#)) was added to illustrate the mounting of the chameleon.
- Collection number of the chameleon was added on [p.4, line 116](#) in the revised manuscript.
- Proper figure plates were created for all the figures in the paper
- All the references were revised and improper updates (DOI) were removed.
- All unIntroduced abbreviations have been addressed by stating what the abbreviation or acronym stands for. CAT scan has been properly introduced on [p. 2, line 30](#) in the revised manuscript.
- All references to TIFF have been corrected.
- The species name has been corrected as can be seen on [p. 4, line 116](#) in the revised manuscript.

I would like to confirm that all co-authors have reviewed this latest manuscript and that they approve submission of this manuscript to GigaScience in its current format. This manuscript has not being submitted elsewhere.

I trust that you would find the manuscript in order and I look forward to hearing from you soon.

Kind regards
Anton du Plessis